BONE SURFACE MICROENVIROMENT MIMICKED BIODEGREDABLE SCAFFOLDS FOR OSTEOGENIC STEM CELL DIFFERENTIATION

by

Birgün Özçolak

B.Sc. in Molecular Biology and Genetics, 2014

Submitted to the Institute of Biomedical Engineering
in partial fulfillment of the requirements
for the degree of
Master of Science
in
Biomedical Science

Boğaziçi University
2016

BONE SURFACE MICROENVIROMENT MIMICKED BIODEGREDABLE SCAFFOLDS FOR OSTEOGENIC STEM CELL DIFFERENTIATION

APPROVED BY:

Assoc. Prof. Dr. Bora Garipcan .....
(Thesis Advisor)

Assoc. Prof. Dr. Albert Güveniş .....

Assist. Prof. Dr. Sedat Odabaş .....

DATE OF APPROVAL: 12 August 2016

ACKNOWLEDGEMENTS

I would like to express my appreciation and special thanks to my advisor Assoc. Prof. Dr. Bora Garipcan. I would like to thank him for encouraging me in my researchs and for inspiring me to become a research scientist. I would also like to thank to my committee members, Assoc. Prof. Dr. Albert Güveniş and Assist. Prof. Dr. Sedat Odabaş. In addition, I would like to give special thanks to my mom, Yeşim Özçolak. I have always have felt their prayers on me during my thesis work. Moreover, I would like to express my appreciation to Selim Akiş who always supported me and helped a lot to finish my thesis. Furthermore, I would like to thank to MSc. Dilara Perver for sharing the same stress during her PhD applications. I would also like to thank Dr. Çağrı Kaan Akkan and M.Sc Onur Arslan for his supporting me in every stage of this thesis. In the end, I would also give my thanks to my laboratory colleagues in developing the project.

This thesis was supported by TÜBİTAK project number 113S730 and I would like to thank TÜBİTAK 2210-C Domestic Graduate Scholarship in Priority Areas for their support.

ACADEMIC ETHICS AND INTEGRITY STATEMENT

I, Birgün Özçolak, hereby certify that I am aware of the Academic Ethics and Integrity Policy issued by the Council of Higher Education (YÖK) and I fully acknowledge all the consequences due to its violation by plagiarism or any other way.

Name :

Signature:

Date:

ABSTRACT

BONE SURFACE MICROENVIROMENT MIMICKED BIODEGREDABLE SCAFFOLDS FOR OSTEOGENIC STEM CELL DIFFERENTIATION

The change of the surface roughness, topography and stiffness as well as the chemical and/or biochemical components of the surfaces; might affect the cell-surface, cell-scaffold interface characteristics and may influence cellular behavior, which are important to investigate new bioprosthesis for tissue engineering applications. Thereby, in this thesis, mimicking bone surface microenvironment was aimed. Firstly, to produce a mould, bovine femur surface was mimicked by using Polydimethylsiloxane (PDMS). A biodegradable polymer, Poly (L-Lactic acid) was poured on the mould to obtain bone surface mimicked (BSM) scaffolds. Then, Bone Morphogenic Protein-2(BMP-2) was loaded on the scaffolds and its release profile was examined in-vitro conditions with Enzyme-Linked ImmunoSorbent Assay (ELISA). BSM scaffolds was modified either with hydroxyapatite (HA) or collagen type-I (Col-I) to construct these scaffolds, similar to the bone‘s natural micro- environment. Modified scaffolds were characterized with Water Contact Angle (WCA) measurements, Scanning Electron Microscope (SEM), X-Ray Photoelectron Spectroscopy (XPS), X-Ray Diffraction (XRD) and Fourier Transform Infrared Spectroscopy (FTIR). Characterization studies were followed by cell culture studies. To analyze cell viability on the scaffolds, MTT was performed. To examine cell proliferation on the scaffolds, Alamar Blue was performed. The effect of the modifications on the controlled and directed osteogenic differentiation in in-vitro conditions was evaluated by using Alkaline Phosphatase Activity analysis, Alizarin Red and SEM EDAX tests.

Keywords: Biomimetic, Bone microenvironment, Bone tissue engineering, Stem cell.

ÖZET

KEMİK MİKROÇEVRE TAKLİT BİYOBOZUNUR DOKU İSKELELERİ İLE OSTJENİK KÖK HÜCRE FARKLILAŞMAŞI

Yüzeyin pürüzlülüğünün, topografisinin ve sertliğinin, bunun yanı sıra yüzeylerin kimyasal ve/veya biyokimyasal içeriğinin değişimi; doku mühendisliği alanında geliştirilecek yeni biyoprotezler için önemli olan hücre-yüzey, ara yüzey karakteristiğini ve hücresel davranışları etkileyebilmektedir. Bu sebeple bu tezde, kemik yüzey mikro-çevresinin taklidi amaçlanmıştır. İlk olarak, kalıp üretebilmek için, sığır femur yüzeyi polimetilsiloksan (PDMS) kullanılarak taklit edilmiştir. Biyobozunabilen bir polimer olan, poli (L-laktik asit) (BSM) doku iskeleleri kemik yüzeyini taklit edebilmek için bir kalıba dökülmüştür. Daha sonra, kemik morfojenik protein-2 (BMP-2) iskeleler üzerine yüklenmiş ve salım profili Enzyme-Linked Immunosorbent Assay (ELISA) ile in vitro koşullarda incelenmiştir. BSM iskeleleri, kemiğin doğal mikro-çevresine benzer iskeleler oluşturulması için hidroksiapatit (HA) ya da tip 1 kolajen (Col-I) ile modifiye edilmiştir. Modifiye doku iskeleleri Su Temas Açısı ölçümü, Taramalı Elektron Mikroskobu (SEM), X-Işını Fotoelektron Spektroskopisi (XPS), X-Işınları Kırınım Cihazı (XRD) ve Fourier Dönüşümlü Infrared Spektrofotometre (FTIR) ile karakterize edilmiştir. Karakterizasyon çalışmalarını hücre kültürü çalışmaları izlemiştir. Doku iskeleleri üzerine ekilen hücrelerin canlılığını analiz etmek için, MTT yapılmıştır. Doku iskeleleri üzerinde hücre çoğalmasını incelemek için Alamar Mavisi yapılmıştır. Modifikasyoların in-vitro koşullarda kontrollü ve indüklenmiş osteojenik farklılaşma üzerindeki etkisi, Alizarin Kırmızı, alkalin fosfataz aktivitesi analizi ve SEM EDAX testleri kullanılarak değerlendirilmiştir.

Anahtar Sözcükler: Biyomimetik, Kemik Mikroçevresi, Kemik doku mühendisliği, Kök Hücre

TABLE OF CONTENTS

LIST OF FIGURES

LIST OF TABLES

LIST OF SYMBOLS

C_{RED}	Concentration of reduced form alamarBlue® (RED)
C_{OX}	Oxidized form of alamarBlue® (BLUE)
ϵOX	Molar extinction coefficient of alamarBlue oxidized form (BLUE)
ϵRED	Molar extinction coefficient of alamarBlue reduced form (RED)
A	Absorbance of test wells
A'	Absorbance of negative control well. The negative control well should contain media + alamarBlue but no cells.
$\lambda 1$	570nm
$\lambda 2$	590nm

LIST OF ABBREVIATIONS

BMPs	Bone Morphogenetic Proteins
ADMSC	Adipose Derived Mesenchymal Stem Cell
TGF-B	Transforming Growth Factor-?
FGF	Fibroblast Growth Factor
IGFs	Insulin-Like Growth Factors
PDGF	Platelet-Derived Growth Factor
VEGF	Vascular Endothelial Growth Factor
PAA	Poly (Acrylic Acid)
PVA	Poly(Vinyl Alcohol)
PHEMA	Poly(2-Hydroxyethyl Methacrylate)
PLA	Poly (Lactic Acid)
PLGA	Poly(Lactic-Co-Glyco-Lide)
PCL	Poly(E-Caprolactone)
PGA	Poly (Glycolic Acid)
3D	Three-Dimensional
Col-I	Collagen Type-I
HA	Hydroxyapatite
BMP-2	Bone Morphogenetic Protein 2
BMP-7	Bone Morphogenetic Protein 7
ELISA	Enzyme-Linked ImmunoSorbent Assay
SEM	Scanning Electron Microscopy
AFM	Atomic Force Microscopy
WCA	Water Contact Angle
XPS	X-Ray Photoelectron Spectroscopy
XRD	X-Ray Powder Diffraction
FTIR	Fourier Transform Infrared Spectroscopy
BSM	Bone Surface Mimicked
IPSCs	Induced Pluripotent Stem Cells

MTT	3-[4, 5-Dimethylthiazol-2-Yl]-2, 5 Diphenyltetrazolium Bromide

1. INTRODUCTION

1.1 Motivation

"Biomimetics" is a term that comes from the Greek words "bios" (life) and "mimesis" (to imitate). It is an inspired usage of technology that imitates the nature to make human lives better. The functions and principles of biomimetic, which could be practiced in biomedical engineering, are originated from various natural events, like the regeneration of the lizard's tail and the regeneration of the buckhorn's horns each year, the phlegmatical, adhesive and regenerative properties of the web of the spider [1]. Thus, in tissue engineering, various hybrid composites, which are inspired by the nature, have been designed as a template in order to control biological processes. For example, some structural biomaterials like nacres or bones have hierarchical construction and organization. So as to mimic these biomaterials' structural complexity, inorganic-organic hybrid materials were used [2]. Furthermore, the occurrence of bone disorders is expected to double by 2020 especially in some populations in which aging is coupled with not only high rate of obesity but also with poor physical activity [3]. Although, bone is able to renew itself, some bone defects whose size is large could be really challenging for the orthopedicians. Bone grafting is a method to treat these large defects as an allograft or an autograft. However, the usage of an allograft or an autograft also has some disadvantages like second-site surgery, donor incompatibility and limitations of available bone tissue [4]. Engineered bone tissue could be a potential alternative to be a conventional bone graft, because of their limitless supply and unfeasibility to transmit disease. With bone tissue engineering applications, inducing new functional bone regeneration with the synergistic combination of cells, factor therapy and biomaterials is aimed [3]. In tissue engineering applications, the usage of the synthetic and biodegradable polymer scaffolds is preferred due to their mechanical properties, biocompatibility, the degradation rate and microstructure [5]. In addition, seeding or growing the cell on the biodegradable polymer scaffold could endorse tissue growth and remodeling [6, 7] and affect cell behaviors like proliferation,

migration, adhesion, and differentiation [8].

Tissue engineering scaffolds should be able to ensure the mechanical support as well as having control over nanoscale topography, architecture and biochemical signals to affect cellular processes. In this context, poly (lactic acid) (PLA)-based biomaterials could be mentioned as a qualified material to invent various regenerative engineering practices in orthopedics field due to their flexible fabrication, biocompatibility and biodegradability [9]. In addition, PLA also have drug loading capacity and its byproducts are non-toxic as well [1].

A stem cell can be defined as an undifferentiated cell, which have multi lineage differentiation and self-renewal capacity without senescence. There are three type of stem cells such as Totipotent stem cells which is able to give rise to a full viable organism, pluripotent stem cells which is able to differentiate into any cell type within in the human body and multipotent stem cells which are able to differentiate into some but not all, cell types. For example, adipose derived stem cells (ADMSC) are multipotent and able to go under osteogenic differentiation [10, 11]. Thus, the usage of the adipose derived stem cells is useful to investigate the biocompatibility of our samples and their affect on osteogenic differentiation [4].

To sum up, altering both the physical structure of the surface such as its roughness, topography and stiffness and its chemical and/or biochemical components; may influence cellular behaviors, which are crucial to investigate new bio prosthesis for tissue engineering applications. Thus, to investigate mimicking physically and biochemically bone surface microstructure to initiate osteogenic differentiation of the stem cells could be a promising technique in bone tissue engineering field.

1.2 Objectives

In this thesis, our aim is mimicking physical, chemical and biochemical structure of the bone and investigating proliferation and differentiation behavior of the ADMSC

on the bone surface microstructure mimicked membranes. In order to mimic bone surface topography, PLA was used as a biocompatible and biodegradable polymer. For mimicking bone's biochemical structure, Collagen Type-I (Col-I) and Hydroxyapatite (HA) was immobilized on the bone surface topography mimicked samples. So as promote osteogenesis of the stem cells; a growth factor, Bone Morphogenetic Protein 2 (BMP-2), loaded into Col-I and HA immobilized bone surface mimicked (BSM) samples. Finally, the effect of the PLA scaffolds on the proliferation and differentiation of ADMSC was examined. The main objectives of this study are:

- To mimic the biochemical structure bone surface microstructure with Col-I and HA immobilization on the biodegradable PLA membranes.
- To examine the release profile of the loaded growth factor, BMP-2 in the PLA membranes with Enzyme-Linked Immuno Sorbent Assay (ELISA) technique.
- To characterize physically and biochemically bone surface microstructure mimicked membranes' by using Scanning Electron Microscopy (SEM), Atomic Force Microscopy (AFM), Water Contact Angle (WCA) Measurement, X-Ray Photoelectron Spectroscopy (XPS), X-ray Powder Diffraction (XRD), Fourier Transform Infrared Spectroscopy (FTIR).
- To investigate viability, proliferation and osteogenic differentiation of the ADMSC on the physically and biochemically BSM PLA scaffolds
- To examine the effect of the BMP-2 loaded scaffolds, on proliferation and osteogenic differentiation of ADMSC.

1.3 Outline

The thesis is presented as follows: In chapter 2, background information about bone and its structure, current bone repair and regeneration methods, stem cell applications and bone tissue engineering are given. In chapter 3, the experimental procedures

are explained. In chapter 4, the results are presented. In the last chapter, the results and their implications as well as the future studies, which would be done, were discussed.

2. BACKGROUND

2.1 Bone

Bone has a fundamental role not only in the movement, support and shape of the whole body but also in the protection of the some organs [12]. It is also significant to mineral storage, homeostasis, blood production, blood pH regulation, regulation of the concentration of the blood electrolytes. In addition, it is also a shelter of the multiple progenitor cells like mesenchymal and hematopoietic cells [13].

2.1.1 Bone Structure

Bone is an extremely diverse and dynamic tissue, not only structurally but also functionally. Distinct loading conditions principally influenced mechanical properties and macroscopic features of the quite two hundred bones within the human skeleton. Skeletal structures have various bone types such as long, short, flat, and irregular. Bone functions vary from vital organ protection to locomotion. Bone tissue might in addition not solely fight a compact (i.e., cortical bone) or fibrous tissue (i.e., cancellous bone) pattern arrangement however additionally gets into mechanical strength and modulus. In spite of those sophisticated options and forms, it's relative simplicity in terms of its microscopic, graded manner. Specifically, as it could be seen at Figure 2.1.1, bone extracellular matrix consists of every a non-mineralized organic part, which contains predominantly Col-I, and a mineralized inorganic half, which comprised of 4-nm-thick plate-like carbonated apatite mineralizes. The nano-composite structure (stiff and multi-pronged albuminoidal fibers supported by hydroxyapatite crystals) is integral to bone's high fracture toughness and its compressive strength [3].

In addition, bone, which is a mineralized connective tissue and contains four kinds of cells, such as osteoblasts, bone lining cells, osteocytes, and osteoclasts [14,15].

Bone carries out necessary functions within the body, like locomotion, support and protection of various kinds of tissues, phosphate and calcium storage, and harboring of bone marrow [16, 17]. Contrary to its inert structure, bone could be an extremely dynamic organ that's unceasingly resorbed by osteoclasts and neoformed by osteoblasts. There's proof that osteocytes act as mechanosensors and orchestrators of this bone remodeling process [18, 19]. The function of bone lining cells isn't explicit, however these cells seem to play a vital role in coupling bone resorption to bone formation [20].

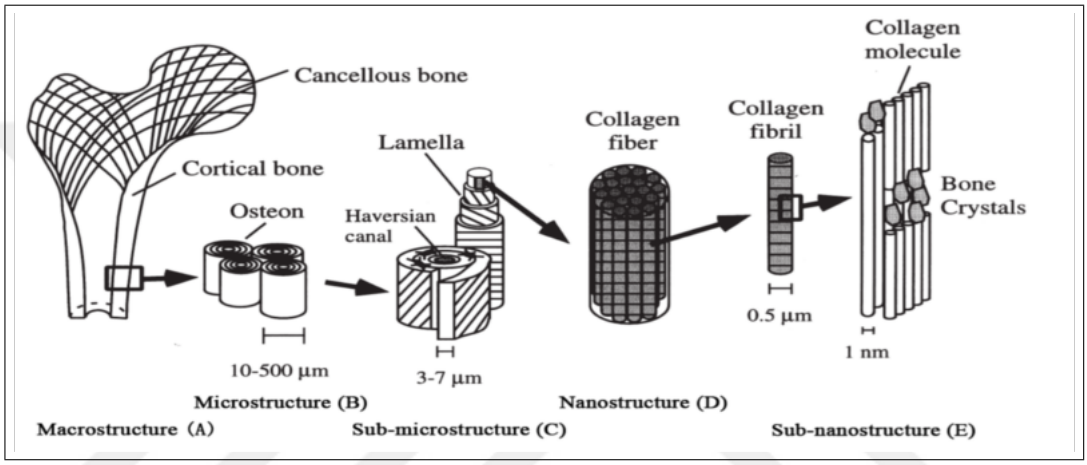

Figure 2.1 Hierarchical structural organization of bone [21]

2.1.2 Bone Regeneration

Cartilage and bone defects occur owing to various reasons like degenerative, traumatic and surgical processes, which notably affect life quality of person. Each year, there are millions of patients, who are suffering from cartilage and bone defects, have approximately 250,000 knee arthroplasty and 450,000 bone grafts in the United States alone [22, 23].

Bone remodeling is an extremely complicated process in which previous bone is replaced by new one. That replacement process is like a cycle, which is comprised of three phases, such as, initialization of bone resorption by osteoclasts, the transition process from resorption to new bone formation, and the bone formation by osteoblasts (Figure 2.1.2) [24, 25]. In addition, this process happens as a result of coordinated

actions of osteocytes, osteoblasts, osteoclasts, and bone lining cells [26–28]

Normal bone remodeling is not only critical to fracture healing and skeleton adaptation to mechanical use, but also important to calcium homeostasis [29]. In contrast, an imparity of bone tissue formation and resorption leads to various bone diseases. For instance, an excessive resorption by osteoclasts without the corresponding quantity of new-formed bone by osteoblasts support bone loss and osteoporosis [30], whereas an excessive bone tissue formation might lead to osteopetrosis [31]. Thus, the equilibration between bone resorption and formation is important and based on the action of many systemic and local factors together with cytokines, hormones, biomechanical stimulation and chemokines [32–34].

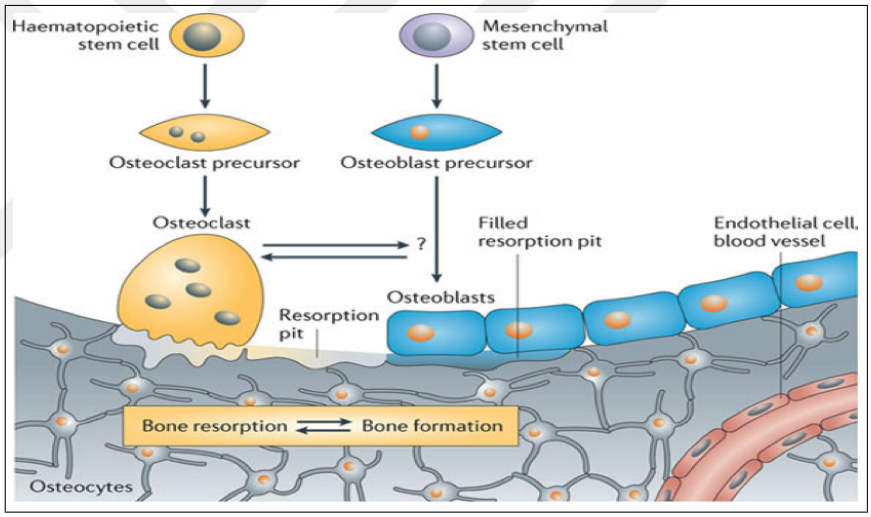

Figure 2.2 Bone Resorption and Formation [35]

2.1.3 Bone Defects Repair Applications

Nowadays, there has been an extremely high demand for functional bone grafts around the world. In the United States, about half million patients need the repairs of bone defect, with a price bigger than $2.5 billion each year. The occurrence of bone disorders is expected to double by 2020 especially where aging is coupled with not only high rate of obesity but also poor physical activity [36]. Although bone is able to renew itself, some bone defects whose size is large could be really challenging for the

orthopedicians. Bone grafting is a method to treat these large defects as allograft or autograft [4].

Up to the present, autografts has been the best method for bone grafts since they are non-immunogenic as well as histocompatible and they also supply all of the imperious properties needed to a bone graft material. Additionally, in order to attain osteogenesis like osteoprogenitor cells, osteoinduction like bone morphogenetic proteins (BMPs) as well as different growth factors, and osteoconduction like three-dimensional matrix as well as porous matrix; autografts own some essential elements. However, autografts also have some disadvantages. For example, they involve gathering bone from iliac crest of the patient. Thereby, patient needs a second operation where tissue harvest was done [37]. In addition, autologous bone transplants are terribly valuable procedures, and they also might lead to vital donor site morbidity [38] and injury, deformity, scarring and they are related to surgical risks as well: infection, inflammation, injury and chronic pain [39, 40].

Allograft, which has been the second most prevalent bone-grafting technique, is inclusive of transplant donor bone tissue and they usually comes from a cadaver. In addition, allogeneic bone is seemingly histocompatible, and it is also accessible in varied forms, such as demineralized bone matrix, cancellous and morcellised chips, cortical grafts and cortico-cancellous, and whole-bone segments and osteochondral, based on the host-site necessities. In contrast to autografts, allografts are related to risks of infection transmission and immunoreactions and the reduction of the osteoinductive properties as well as cellular parts are required for them. Thus, donor grafts are devitalized via irradiation or lyophilization process [41–43]. However like autografts, allogenic grafts has also substantial cost issues [44]. Another widely used bone repair technique is xenograft, which is obtained from one species and transplanted into another and has the same limitations that allografts have [45]. Thereby, tissue engineering applications could be accepted as a possible alternative therapeutic process to cure rigorously injured patients.

2.2 Bone Tissue Engineering

Tissue Engineering, which focuses on to design functional three-dimensional (3D) tissues combining scaffolds, cells and/or bioactive molecules, is an interdisciplinary field [46]. Since, this field includes various scientific areas like engineering, material science, cell biology, molecular biology, chemistry and medicine. In 1993, the Tissue Engineering term, which was firstly defined by Langer and Vacanti, is still in used and indicates that the fundamental aim in Tissue Engineering is the improvement of biological substitutes to restore, improve or maintain tissue function [8]. Thus, Tissue Engineering could be able to avoid tissue damage related problems of the existing treatment methods like mechanical devices, transplants or surgical reconstruction. For example, organ transplants show important limitations such as lack of donor and rejection of the transplant. In addition, mechanical devices could not be able to avoid the progressive deterioration of patient and achieve each the function regarding to the tissue. Lastly, surgical reconstruction could be caused long-term problems [47]. Thus, Tissue Engineering originate in the requirement of the more absolute solutions in order to repair tissue in clinics and also it purposes to succeed this goal with the improvement of the in vitro devices, which would restore in vivo damaged tissue.

2.2.1 Biomaterials For Tissue Engineering

There are several definitions have been used to the term "biomaterials" such as, it is a "material exploited in contact with living tissues, organisms, or microorganisms" [48] and "a substance that has been engineered to take a form which, alone or as part of a complex system, is used to direct, by control of interactions with components of living systems, the course of any therapeutic or diagnostic procedure, in human or veterinary medicine" [49]. In general, biomaterials are contemplate to interface with biological systems to replace, treat, augment or evaluate any function, tissue or organ of the body and also they are in use for several different treatment applications. The main difference between biomaterials and other materials is that biomaterial is able to endure in a biological environment as well as it is damaged in that process and it does

not damage the surroundings.

Naturally derived materials, polymers, composites and ceramics could be used as biomaterials. Natural biomaterials could be comes from individuals of the same species (allografts), from different species (xenografts) or from the same individual (autografts). Furthermore, ceramic materials depend on bioglasses and calcium phosphates. Although they have well osteoinductive properties, they have difficulties in forming procedure and their mechanical properties are low. Polymers like those derived from PLA and polyglycolic acid (PGA) have biodegradability, good mechanical properties, easy formability and they also vary regarding to their molecular weight. However they do not have good osteoinductive properties. Thus, ceramic-polymer composite materials enable scientists to produce a biodegradable material, which have osteoconductive, osteoinductive, conformability and good mechanical strength properties [50].

2.2.2 Synthetic Polymeric Biomaterials in Bone Tissue Engineering Applications

As a scaffold material, which was used in tissue engineering, the synthetic or natural polymers such as, poly (a-hydroxy ester), polysaccharides, thermoplastic elastomers or hydrogels were the most popular ones [51]. Synthetic polymers are easy processable, available, mechanically stabile for a long time and also they are cytocompatible due to their chemical and mechanical properties. There are two type of synthetic polymers such as, biodegradable and non-degradable polymers. PLA and PGA, poly(lactic-co-glyco-lide) (PLGA), poly(e-caprolactone) (PCL), poly(carbonate)s, poly(fumarate)s, poly(anhydride)s, poly(urethanes), poly-α-hydroxy esters poly(orthoester)s, poly(hydroxyalkano- ate)s, poly(phosphazene)s were the widely used biodegradable polymers. However, there are some main disadvantages of the synthetic polymers, such as, these biomaterials are innate hydrophobic and they have concomitant inefficient cellular interaction and attachment.

On the other hand, the usage of the non-degradable polymers such as poly (acrylic acid) (PAA), poly(vinyl alcohol) (PVA), poly(2-hydroxyethyl methacrylate) (PHEMA) are still limited. They are mostly used in permanent implants or low molecular weight blocks to enable degradation in the body [52].

2.2.3 Growth Factors and Repair

The growth factors could be able to stimulate gene expression, cellular adhesion, proliferation, differentiation and migration. With the extracellular domain's binding to a target growth factor receptor, the intracellular signal-transduction, which finally goes to the nucleus and causes the mRNA transcription and the respective proteins' synthesis, is activated [53–55].

Single growth factors could be able to have effects on several cell types and may stimulate different functions. In order to stimulate an intracellular signal transduction, growth factors bind to cell's target cell receptors. Then, signals go to the nucleus to determine the biological response (Figure 2.2.3).

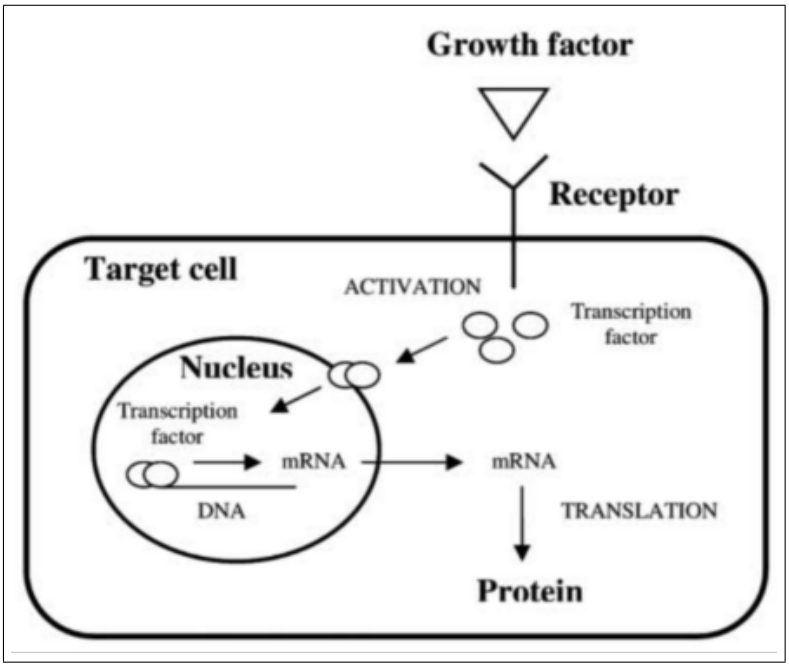

Figure 2.3 The growth factor mechanism on cellular activity [56].

The major growth factors acting on the skeleton are transforming growth factor-β (TGF-β), BMPs, fibroblast growth factor (FGF), insulin-like growth factors (IGFs), platelet-derived growth factor (PDGF) and vascular endothelial growth factor (VEGF). In bone repair process, bone microenvironment cells like inflammatory cells, endothelial cells, fibroblasts, osteoblasts and bone marrow stromal cells (BMSC) generate growth factors [57,58]. The osteoprogenitors' migratio is increased by BMPs, FGF, PDGF and VEGF. The periosteum-derived cells' proliferation is initiated by FGF and PDGF [59]. Differentiation and proliferation of the osteoprogenitor cells is moderated by IGFs, TGF-β, BMP-2, BMP-6, and BMP-7. In addition, vascular ingrowth into bone is controlled by FGF-2 and VEGF [56].

Nowadays, clinical use of the growth factors is limited because appropriate delivery systems haven not been developed yet [60]. Firstly, an ideal delivery system, which is designed to repair bone, would combine osteoinductive and osteoconductive properties. In addition, the ideal delivery device would provide a scaffold that improves cell attachment as well as cell recruitment, provide the bioactive growth factor's time and dose-controlled release, and assign required space to endorse angiogenesis as well as cell migration. Finally, a carrier, which is used to deliver growth factor, should be adequately biodegradabile, highly biocompatible, mechanically congruent, malleable, non-toxic, cost effective and easily manufactured [61].

2.3 Stem Cells and Their Usage in Bone Tissue Engineering Applications

Cell source selection to design tissue engineering strategies is an important decision for the clinical applications. The cells, which were used in tissue engineering applications, should integrate to the specific tissue in order to secrete several cytokines and growth factors, which activate the regeneration program of the endogenous tissue. The usage of some cell types can cause inherent difficulty in some specific cell types' growth. Thus, stem cells either Adult stem cell or embryonic stem cell have arisen

as favorable alternative cell sources [62]. Embryonic stem cells, which are pluripotent cells, have ability to differentiate into any lineage. However the usage of them is highly limited due to ethical arguments and their teratomas production potential [63].

Induced Pluripotent Stem Cells (iPSC), which were created by Yamanaka et al. by using mouse fibroblasts, could be an alternative as a source of cell for tissue engineering applications [64, 65]. iPSC are somatic cells which are reprogrammed to get into a pluripotent state by introducing a set of transcription factors. Although these cells have autologous character, good differentiation capacity and also simple reprogramming procedure, there are various barriers to achieve before widely usage of iPSC [66, 67].

ADMSC, which could effortlessly be isolated from adipose tissue, are mesenchymal stem cells. In 2001, they were first defined by Zuk et al. as a population of cells, which is capable of multilineage differentiation, obtained from human adipose tissue. Like other stem cell types, ADMSC has ability to differentiate into other cell types and renew itself [68]. In embryonic period, adipose tissue pertains to the mesodermal layer [69] and is composed of a stromal vascular fraction and adipocytes [70, 71]. At first, it was thought that the differentiation of ADMSC was supposed to be restricted to mesodermal tissue only. However, recent studies demonstrated that ADMSC have an extend usage from mesodermal and ectodermal tissues to organs [72]. More recent studies have discovered that ADMSC have a several differentiation pathways,like adipogenesis, osteogenesis, chondrogenesis, and other lineages.

Although bone marrow-derived stem cells are the most widely used adult stem cells ADMSC have many benefits over them. The first advantage of the ADMSC is its extracting procedure. Even though the procedure, which is used to extract BMSCs, is actually painful, and also its effectiveness in terms of the cell yield rate is quite low [73], ADMSC have plentiful sources, which are located in subcutaneous adipose tissue and obtaining ADMSC using the minimally invasive liposuction is quite easy, and its yield percentage is fairly better than other stem cell resources [74]. Furthermore, ADMSC could be transplanted into allogeneic or autologous body safely with fewer foreign body

reaction and implant migration [75]. Thereby, ADMSC have become the most effective stem cell source in tissue engineering field.

3. MATERIALS AND METHODS

3.1 Preparation of Bone Surface For Mimicking

In order to prepare BSM scaffolds, bovine femur, which was bought from a local butcher, was used after cutting it into small pieces with a bone saw. To clean these bone pieces, the xenograft cleaning procedure was applied (Figure 3.1) [76, 77]

In this xenograft cleaning process, osmotic bath (ultrasonic bath), oxidative and alkaline processes were applied. In this process, to remove the remaining cells and tissue particles on the bone, bone pieces were put into the 10% NaCI solution for 24 hours and first 20 minutes of this process was done into ultrasonic bath. To get rid of remaining lipids from the surfaces of these bones, the acetone bath process was also used. In order to deterge the immunologic structures, bones treated with 3% H_2O_2 and to increase the effectiveness of this step, the first and last 5 minutes of this process was applied into ultrasonic bath. Finally, for the inactivation of the prions, which are harmful for collagen and inorganic structure of bone, 2N NaOH was used as well as the first 15 minutes of this process was applied into ultrasonic bath.

3.2 Preparation of PDMS Molds For Mimicking Bone Surface Topography Microstructure

Following bone cleaning procedure, bone surface topography mimicked by using PDMS (Sylgard 184; Dow Corning, Midland, MI) via soft lithography technique. PDMS with 10:1 mass ratio was prepared by mixing silicon elastomer with curing agent in a cup and then, the cup was placed in a dessicator to degas, in other words to remove the gas from the solution. Then, the PDMS was poured on bone surface or plain surface and placed in an oven for 4h at 70C°. The PDMS was used as a mold in order to transfer the bone surface topography to a biodegradable polymer PLA [76].

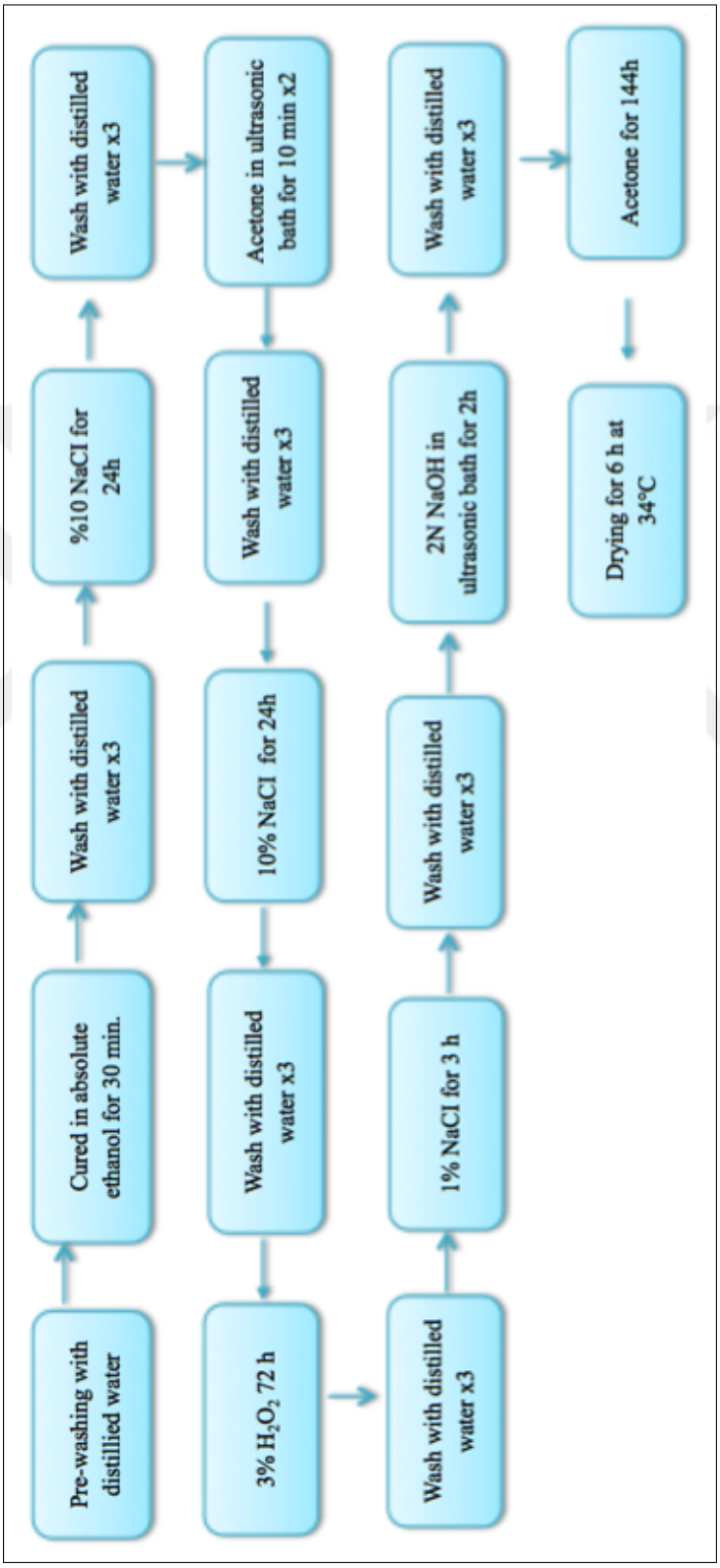

Figure 3.1 Xenograft cleaning process [76, 77].

3.3 Preparation of Plain and BSM PLA Scaffolds

The PDMS molds were used to produce bone surface mimicked PLA scaffolds. In order to prepare these PLA scaffolds, 10% (w/v) PLA in chloroform was prepared and poured onto these molds and the casting time of this procedure is 12 hours (Figure 3.2) [76].

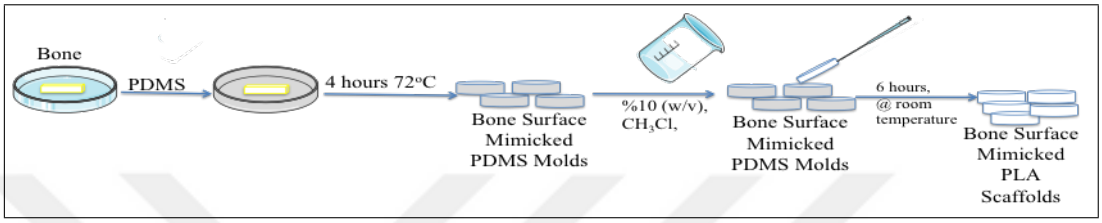

Figure 3.2 Preparation of Bone Surface Mimicked PLA Scaffolds.

3.4 Modification of Plain and BSM PLA Scaffolds

In order to load growth factor in the scaffolds to increase the osteogenic differentiation, BMP-2 was loaded into each BSM PLA scaffolds and so as to chemically mimicking the microstructure of bone. 15 ng BMP-2 protein was added into the 10% (w/v) PLA in chloroform solution. PLA-BMP-2 solution was poured onto these molds and again the casting time of this procedure was 12 hours. Finally the release profile of BMP-2 was examined at in-vitro conditions, in PBS, which includes 1% Bovine Serum Albumin (BSA), 10 mg/ml Heparin and 1 mM EDTA at 37C°.

To mimic bone microstructure biochemically, BMP-2 loaded PLA scaffolds were also modified with HA or Col-I (Figure 3.3). To modify these scaffolds with HA, the scaffolds were activated with O2 Plasma Treatment at 100 W Power, 80 Pa Pressure for 10 minutes. Then, the scaffolds were immersed into 50 ml of 1% (w/v) HA in ethanol suspension for 1 hour at room temperature under stirring [78]. In order to perform Col-I modification, scaffolds were activated with O2 Plasma Treatment at 100 W Power, 80 Pa Pressure for 10 minutes. Then these scaffolds were incubated into

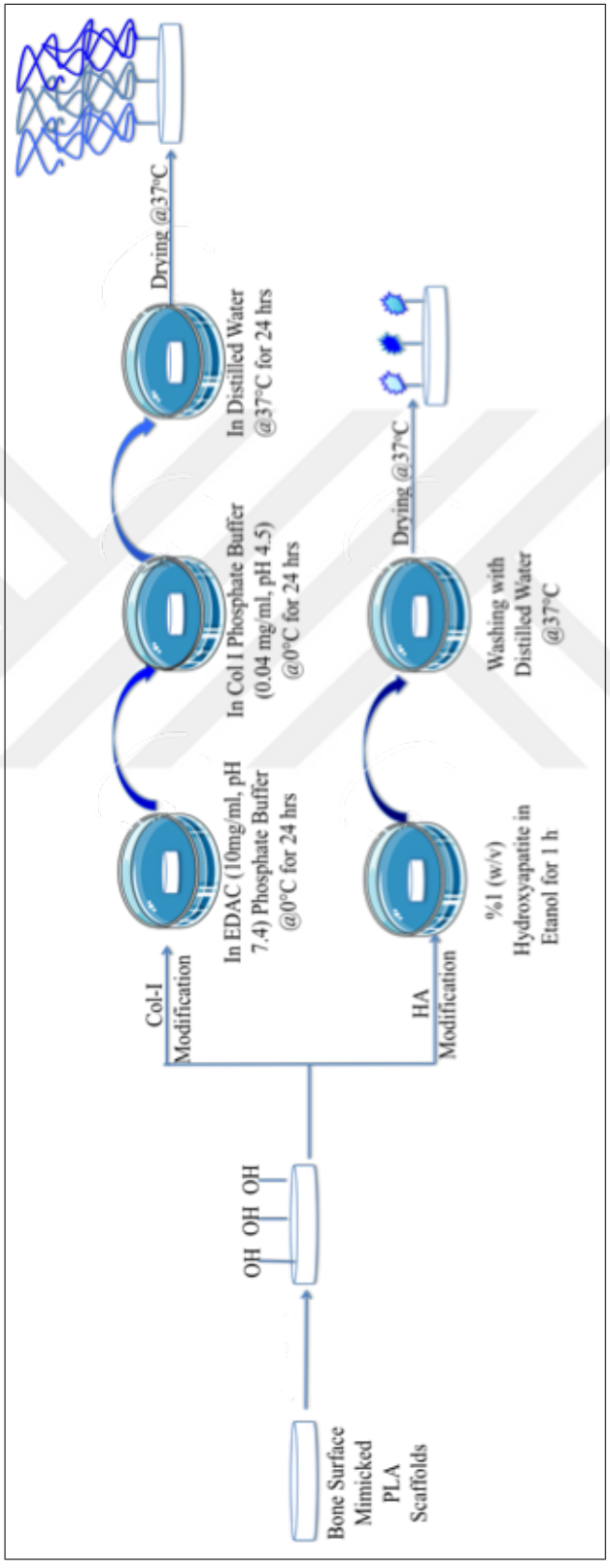

Figure 3.3 Col-I and HA Modifications of PLA Scaffolds.

EDAC Phosphate Buffer solution (10 mg/ml, pH 7.4) for 4 hours at 0C° to activate the COOH residues on the surface of the scaffolds. Finally, these scaffolds were transferred into the phosphate buffer solution (pH 4.5), which includes 0,04 mg/ml Col-I [79].

3.5 Surface Characterization of Bone, PDMS and PLA Scaffolds

3.5.1 Scanning Electron Microscopy (SEM)

Surface topography of chemically modified and unmodified Plain PLA and BSM PLA were examined via Scanning Electron Microscopy (SEM) (Philips XL30 ESEM-FEG/EDAX) at Bogazici University Research and Development Center Electron Microscopy and Microanalysis Unit. All surfaces were coated with thin layer platinum, whose thicknesses are around 50 nm, and then SEM images were taken. SEM was used to observe the success of the Col-I or HA modifications.

3.5.2 Water Contact Angle (WAC) Measurements

Surface WCAs of HA or Col-I modified and unmodified Plain PLA and BSM PLA was measured to take cognizance of the wettability of the scaffolds. The contact angle measurements were performed at Bogazici University Chemical Engineering Department by using contact angle measurement device (DSA 100, Krüss GmbH, Germany) with 10μl/min dosing rate and 10μl initial drop volume. All measurement was performed at room temperature.

3.5.3 Fourier Transform Infrared Spectroscopy (FTIR)

FTIR spectra were recorded over the range of 4000 to 650 cm^{-1} with 32 scans in order to investigate the chemical compositions of unmodified PLA, HA modified PLA

and Col-I modified PLA scaffolds. The FTIR measurements were perfomed at Yıldız Teknik University Department of Chemistry by using Attenuated Total Reflectance Fourier Transform (ATR- FTIR) spectrophotometer (Perkin Elmer, Spectrum 100).

3.5.4 Atomic Force Microscopy (AFM)

In order to investigate the surface roughness value of the scaffolds whose diameter is 15.6 mm^2 was stuck on metal disk by a double-sided cellophane tape at first. Then, the surface roughness of the HA or Col-I modified and unmodified Plain PLA and BSM PLA scaffolds was characterized via AFM in non-contact mode. The measurements were performed at Hacettepe University Department of Chemistry by using AFM (Nanomagnetics Veeco 5A).

3.5.5 BMP-2 Loading and Its Release Profile

PLA was dissolved in CHCI3 at a concentration of 10% and a BMP-2 (15ng per scaffold) (Sigma Aldrich, United State) was added to the solution until the homogeneous mixture was obtained. Then growth factor/polymer solution poured onto PDMS in order to cast BSM as well as growth factor loaded PLA scaffolds. Additionally, plain growth factor loaded PLA was synthesized by using plain PLA and with the same procedure. Growth factor release profile of both scaffolds was measured by using ELISA reader (Bio-rad, iMark micro-plate reader).

The wavelength was read at 450 nm for BMP-2 maximum absorbance. For the growth factor release studies, scaffolds were put into 2 ml phosphate buffer saline (PBS) solution, which includes 10 mg/ml Heparin and 1 mM EDTA, at 37C° with 150 rpm and the growth factor release measurements were performed at 2nd, 4th days and 1st, 2nd, 3rd and 4th weeks at 37C° and 150 rpm [80]. The result of the each experimental group was the average of six parallel measurements, expressed as mean, ± were used to state the standard deviation of these groups. The calibration curve for BMP-2 was

given in Appendix A.

3.5.6 X-ray photoelectron spectroscopy (XPS)

The compositions of unmodified and Col I modified scaffolds were characterized by X-ray photoelectron spectroscope (X-ray Photoelectron Spectrometer, Thermo Scientific K-Alpha), with Al K-radiation (photon energy 1476.6 eV) excitation source and the binding energy of Au (Au 4f7/2: 84.00 eV) was used as a reference [81].

3.5.7 X-ray Diffraction (XRD)

The compositions of unmodified and HA modified scaffolds were characterized by X-ray diffraction (XRD, D/max-2500X) with monochromated Cu Kα radiation (λ 1/4 1.5405 Å, 120 mA, 40 kV) in a continuous scan mode and its scanning speed of 81/min as well as the 2θ range was from 10 to 70 [82].

3.6 Cell Studies

In this thesis, Adipose Derived Stem Cells will be used to see the effect of surface properties on viability, proliferation and osteogenic differentiation.

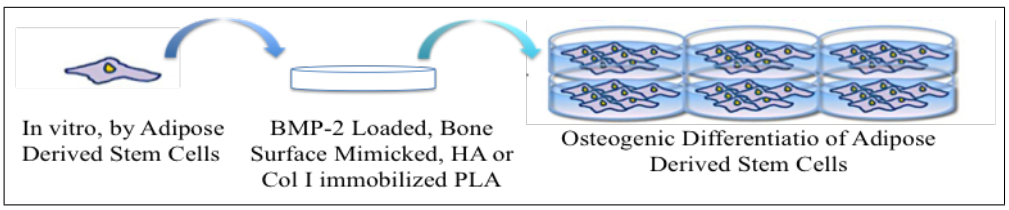

Figure 3.4 Experimental Steps of the cell culture analysis.

3.6.1 The Culture of Human ADMSC

ADMSC at passage 1 (frozen sample) were cultured in growth medium, MesenPRO RSTM Basal Medium (Invitrogen) consisting of %2 MesenPRO RSTM Growth Supplement (Invitrogen), 2 mM L-glutamine (Invitrogen) and 5 μg/ml of gentamicin (Gibco) at 37C° in a humidified incubator (5% CO_2). The medium was changed twice a week. When the cells were reached 80-85% confluence, cells were trypsinized (Gibco Invitrogen). At passage 4, ADMSC were seeded on modified and unmodified PLA surfaces with growth medium. In order to provide the attachment of the cells, there were 3 days of preincubation period for these cells in the growth medium. After preincubation period, half of the growth medium is shifted with differentiation medium which consist of DMEM (Sigma), 10% Fetal Bovine Serum (FBS) (Sigma), 1% Pennicilin (sigma) 10^{-7} M Dexametasone (Sigma) 10 nM β-Glycerophosphate (Sigma), 50 mg/ml of Ascorbic Acid (Sigma) [83]. Every other day, half of the medium was replaced with the fresh medium.

For the each analysis except cell attachment and morphology analysis by using SEM, $2x10^4$ cells were seeded per 24-well plate and for cell attachment and morphology analysis by using SEM, $5x10^3$ cells were seeded per 24-well plate as well.

3.6.2 Cell Viability

The viability of ADMSC was determined by 3-[4, 5-Dimethylthiazol-2-yl]-2, 5 Diphenyltetrazolium Bromide (MTT) assay. The assay exhibits a mitochondrial dehydrogenase activity, which turned light yellow MTT to dark blue Formazan. The photometric measurement of the color change intensity was measured [84]. The samples were incubated at 37C° and in 5% CO_2 atmosphere for different time periods such as 1 day, 4 days, 7 days, 2 weeks, and 4 weeks. During MTT test, the culture medium of the samples was taken and samples were washed by using PBS and then MTT (5 mg/mL) in PBS were added to the culture wells and incubated at 37°C and 5% CO_2 for 3 and half hours. Finally the medium was taken gently and in order to

solve intracellular Formosan 200μl of DMSO (Merck, Germany). The absorbance value of the obtained Formosan was read at 570 nm with a microplate reader (Bio-rad, iMark micro-plate reader) [85]. The experiment was repeated three times, the results of which are presented as means.

3.6.3 Cell Proliferation

In order to perform quantitative cell proliferation measurement, AlamarBlue (Sigma-Aldrich) cell proliferation is used [85]. After incubation for 1 day, 4 days, 7 days, 2 weeks, and 4 weeks, the culture medium of the samples was replaced with the fresh culture medium, which was supplemented with 10 vol.% AlamarBlue fluorescent dye. After that, samples were incubated at 37C° and in 5% CO_2 atmosphere. 100-L culture medium-Alamar Blue solutions from each well were taken so as to read the absorbance value of the samples was read at a wavelength of 570 nm and 595 nm by using a microplate reader (BIO-RAD iMark, Microplate Reader). 10% AlamarBlue fluorescent dye with cell medium without cells is used as a negative control. According to the manufacture's protocol, cell proliferation was obtained by calculating the reduction percentage of alamarBlue with the equations written below:

$$\%Reduced = C_{RED}TestWell/C_{OX}NegativeControlWell \tag{3.1}$$

$$\frac{(\epsilon OX)\lambda 2A\lambda 1 - (\epsilon OX)\lambda 1}{A\lambda 2(\epsilon RED)\lambda 1A'\lambda 2 - (\epsilon RED)\lambda 2A'\lambda 1}X100 \tag{3.2}$$

where are $\epsilon\lambda 1$ and $\epsilon\lambda 2$ constants and represent the AlamarBlue's molar extinction coeffcient. ϵOX is the oxidized form of the AlamarBlue at 570 as well as ϵRED reduced form of the AlamarBlue at 595nm. Absorbance values of test wells are represented as A$\lambda 1$ and A$\lambda 2$ at 570 and 595 nm, respectively. Absorbance values of the negative control wells are represented as A'$\lambda 1$ at 570 nm and A'$\lambda 2$ at 595 nm.

3.6.4 Cell Differentiation

3.6.4.1 Alizarin Red S Analysis

At day 14, 21, 28 Alizarin RedS staining was performed to determine the presence of the calcified extracellular matrix deposits. In order to perform this analysis, the samples were fixed 10% neutral buffer formalin for 25 minutes and then they were rinsed with distilled water for 2-3 times. After that 1 ml of fresh 2% Alizarin RedS solution (pH=4.1-4.3) was added into each well and the samples were incubated for 1 hours. Finally the Alizarin RedS solution was taken from each well, the scaffolds were rinsed with deionized water for 3-4 times. With the increase of the calcification ratio the color scaffolds were turn into red. By using microscopy, the pictures of the samples were taken to identify the red color intensity of the samples [86].

3.6.4.2 Alkaline Phosphatase Activity Analysis

After 7, 14 and 21 days of incubation, samples were the alkaline phosphatase (ALP) activities of the samples were measured by using a BioVision ALP activity kit according to the manufacturer's protocol (Mountain View, CA). In this measurement a microplate reader (BIO-RAD iMark, Microplate Reader) was used to measure the optical density of samples at 540 nm [87].

3.6.4.3 Scanning Electron Microscope (SEM) Analysis

After 28 days of incubation, the medium was taken from the scaffolds, the scaffold were rinsed with PBS two times and the cells on these were fixed by incubating them into 2,5% Gluteraldehyde (Sigma) for 20 minutes. Then, in order to dry the prepared scaffolds for SEM analysis, these were fixed and dehydrated for 2 min each time in increasing concentrations of ethanol in water (30%, 50%, 70%, 90% and 100%); afterwards, they were immediately dried with a Hexamethyldisilazane solution for 5

min [88, 89]. Following this, the samples were coated with thin layer of platinum, whose thicknesses are around 50 nm, and observed under SEM at 10 kV.

3.6.5 Statistical Analysis

Statistical significance was evaluated based on unpaired t-test and one way ANOVA; value of $p<0.05$ was considered significant.

4. RESULTS

4.1 Characterization of the Modified Scaffolds

4.1.1 Scanning Electron Microscopy (SEM)

Due to bone regeneration and modeling arise on the bone surface [90], bone surface morphology is crucial, during bone healing process [91]. In previous studies, it was proved that it is possible to mimic bone surface topography by using bone itself [76]. However, mimicking only the bone surface topography could not be enough to mimic bone microenvironment. Thereby, in this thesis, mimicking both bone surface topography and its biochemical structure were aimed. In order to mimic bone biochemical structure, the PLA scaffolds were modified with Col-I or HA. The surface properties of the Col-I or HA modified or unmodified plain and BSM scaffolds were investigated by using SEM. The surface topography images of the modified and unmodified PLA scaffolds were given in Figure 4.1, 4.2 and 4.3.

According to these images, it could be concluded that BSM scaffolds were mimicked bone surface successfully because the results that we obtained were similar to the previous studies done in our laboratory [76]. In addition, HA particles (Sigma), which had 200 nm particle size in average, were observed on the surface of the HA modified scaffolds. In addition, Col-I, which assembles into fibrils, and has gap regions due to the staggered arrangement, was examined on the surface of the Col-I modified scaffolds [92]. Thereby, these SEM images confirmed the success of the HA and Col-I immobilization on the scaffolds.

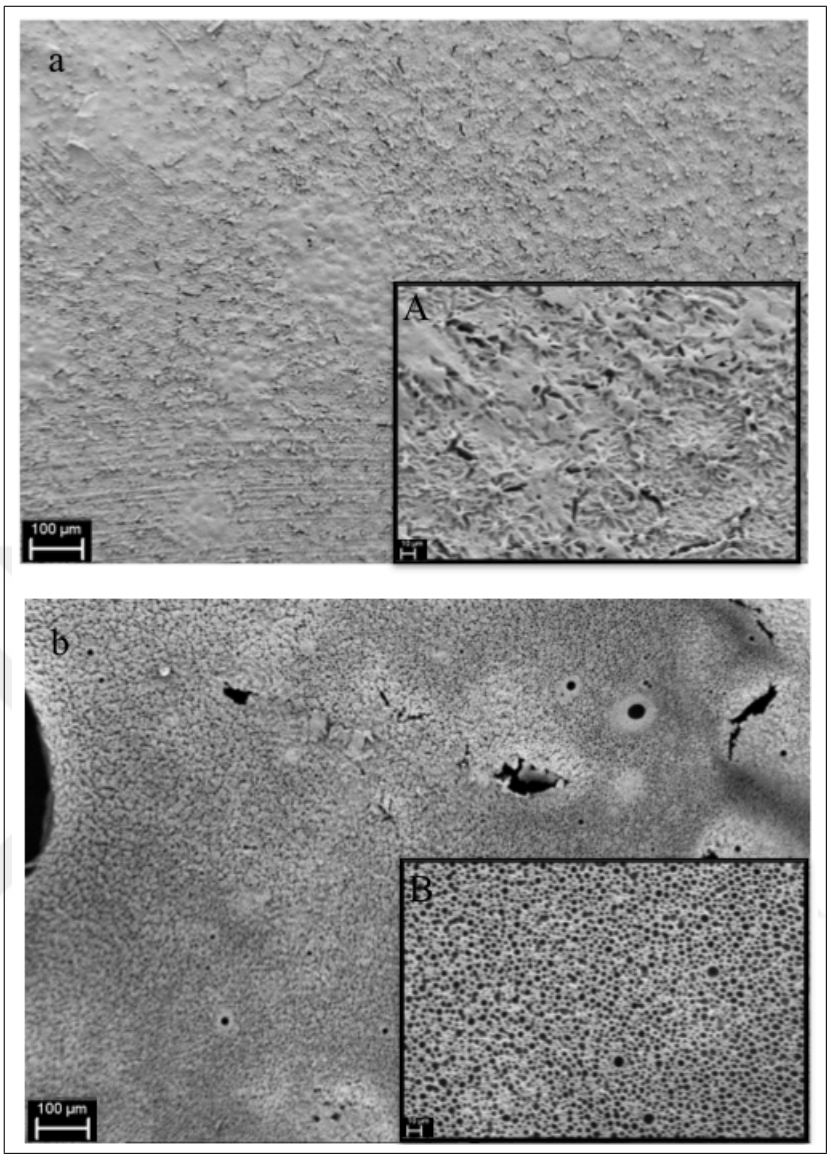

Figure 4.1 SEM surface images of the unmodified Plain and BSM PLA scaffolds with 1000X (inset 10000X) magnification. a) Plain PLA; b) BSM PLA.

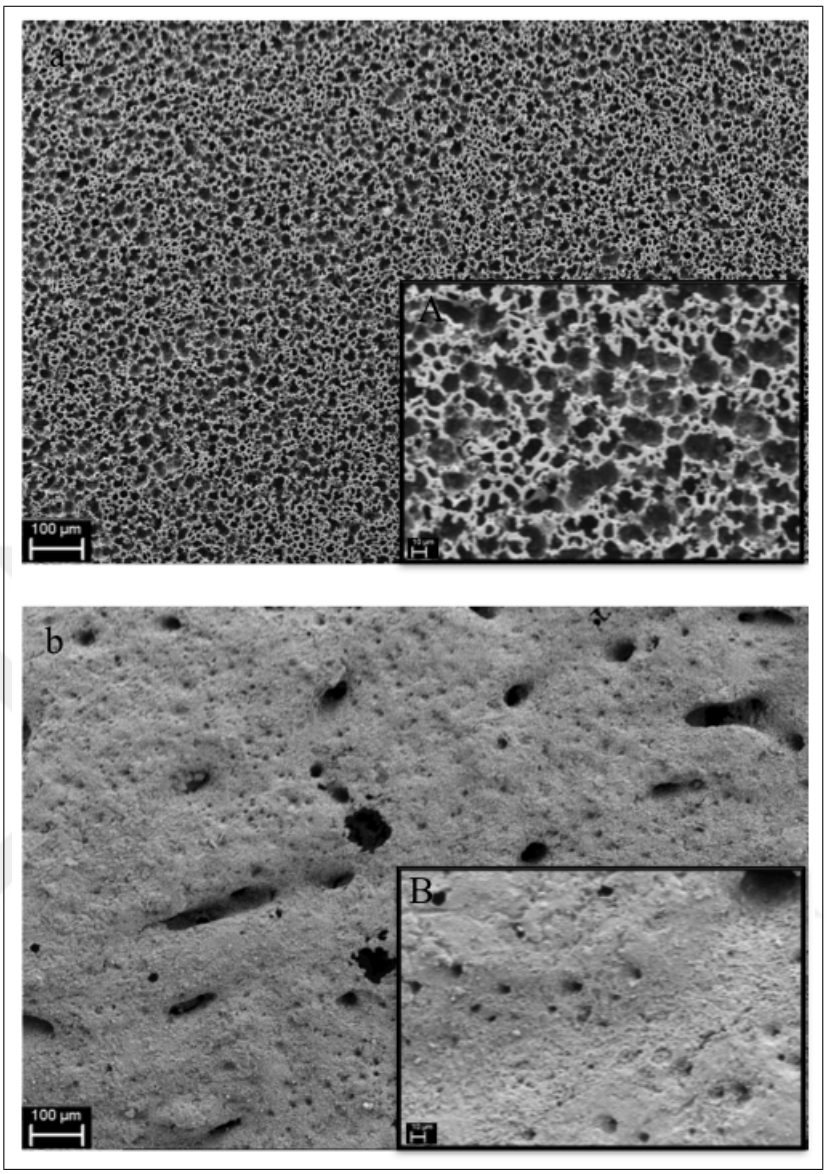

Figure 4.2 SEM surface images of the Col-I modified Plain and BSM PLA scaffolds with 1000X (inset 10000X) magnification. a) Col-I Modified Plain PLA; b) Col-I Modified BSM PLA.

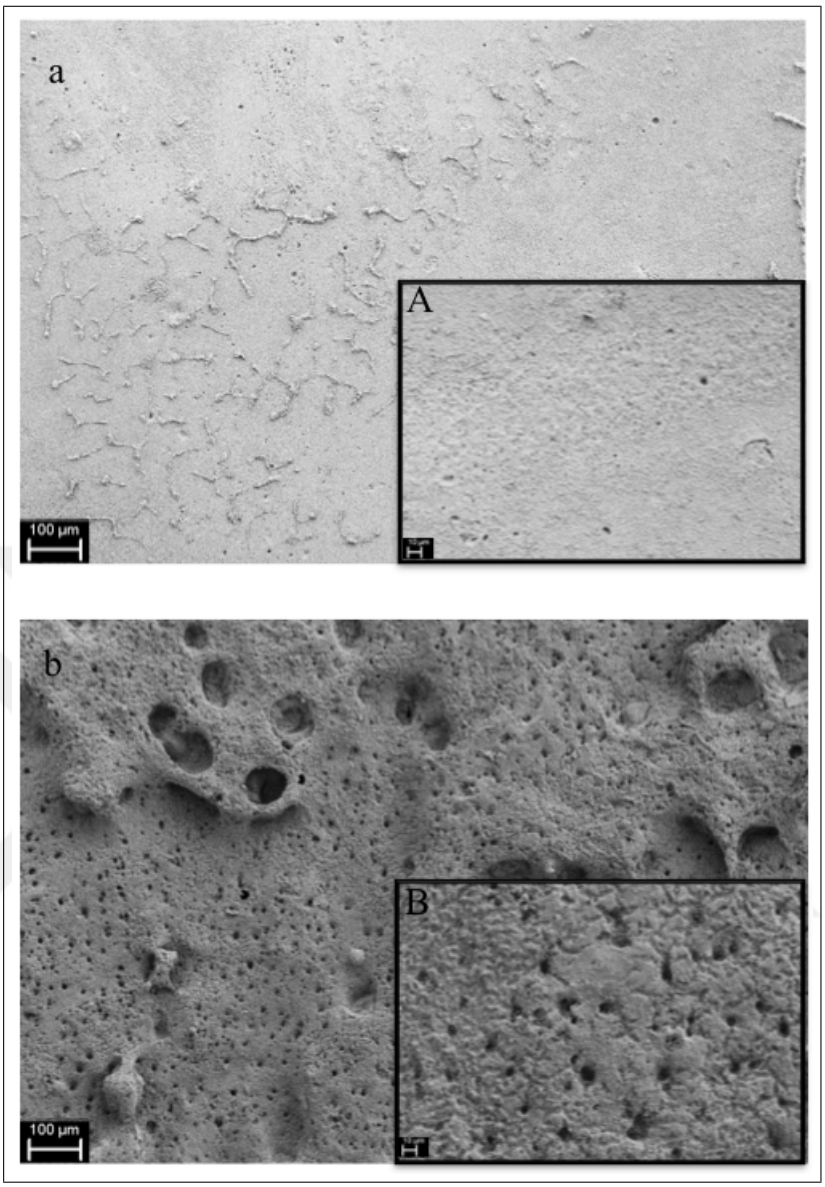

Figure 4.3 SEM surface images of the HA modified Plain and BSM PLA scaffolds with 1000X (inset 10000X) magnification. a) Col-I Modified Plain PLA; b) HA Modified BSM PLA.

4.1.2 WCA Measurements

The wettability of the surfaces has an effect on cell behavior like its adhesion, proliferation and differentiation [93]. In order to observe the wetting properties of the modified and unmodified Plain and BSM scaffolds, the static WCA measurements were performed and the results were given at Table 4.1 and Figure 4.4. According to these measurements, BSM PLA scaffolds were found to be more hydrophobic than Plain PLA

scaffolds and their WCA are 110.44 ± 13.21° and 101.68 ± 7.68°, respectively. The hydrophilic property of the HA or Col-I modified samples was higher than unmodified samples. WCAs of the HA modified Plain PLA and BSM PLA scaffolds were found to be 33.39 ± 5.07° and 18.90 ± 4,61°, respectively. WCAs of the Col-I modified Plain PLA and BSM PLA scaffolds were 49.86 ± 2.24° and 25.84 ± 3.94°, respectively. In addition, the BSM HA or Col-I modified samples were more hydrophilic than plain HA or Col-I modified scaffolds.

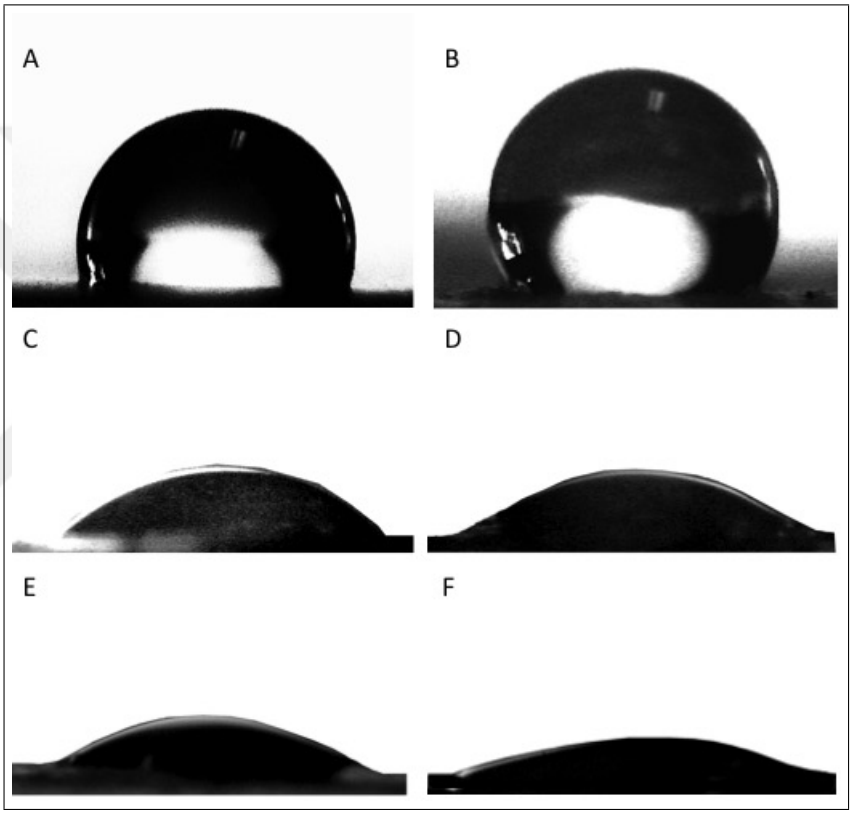

Figure 4.4 WCA images of Modified and Unmodified Plain and BSM PLA scaffolds A) Plain PLA; B) BSM PLA; C) Col-I Modified Plain PLA; D) Col-I Modified BSM PLA; E) HA Modified Plain PLA; F) HA Modified BSM PLA.

Table 4.1
WCA Measurements of Modified and Unmodified Plain And BSM PLA Scaffolds.

Samples	Water Contact Angle(°)
Plain PLA	101.68 ± 7.68
BSM PLA	110.44 ± 13.21
HA Modified Plain PLA	33.39 ± 5.07
HA Modified BSM PLA	18.90 ± 4,61
Col-I Modified BSM PLA	49.86 ± 2.24
Col-I Modified BSM PLA	25.84 ± 3.94

4.1.3 X-Ray Diffraction (XRD) Analysis

In order to prove the immobilization of the HA on the surfaces of the modified scaffolds, Pure HA powder, HA modified PLA scaffolds and unmodified PLA scaffolds, static XRD Analysis was performed. The results were given at Figure 4.5. The broad and small peaks at around $2\theta = 31.7°$ and $2\theta = 32.9°$ are characteristic of HA were observed in the XRD patterns of HA modified PLA scaffolds and Pure HA powder [94–96]. In contrast, no mineral-related peaks were observed for the unmodified PLA membranes. Thereby, it could be suggested that the HA was successfully immobilized onto the PLA scaffolds.

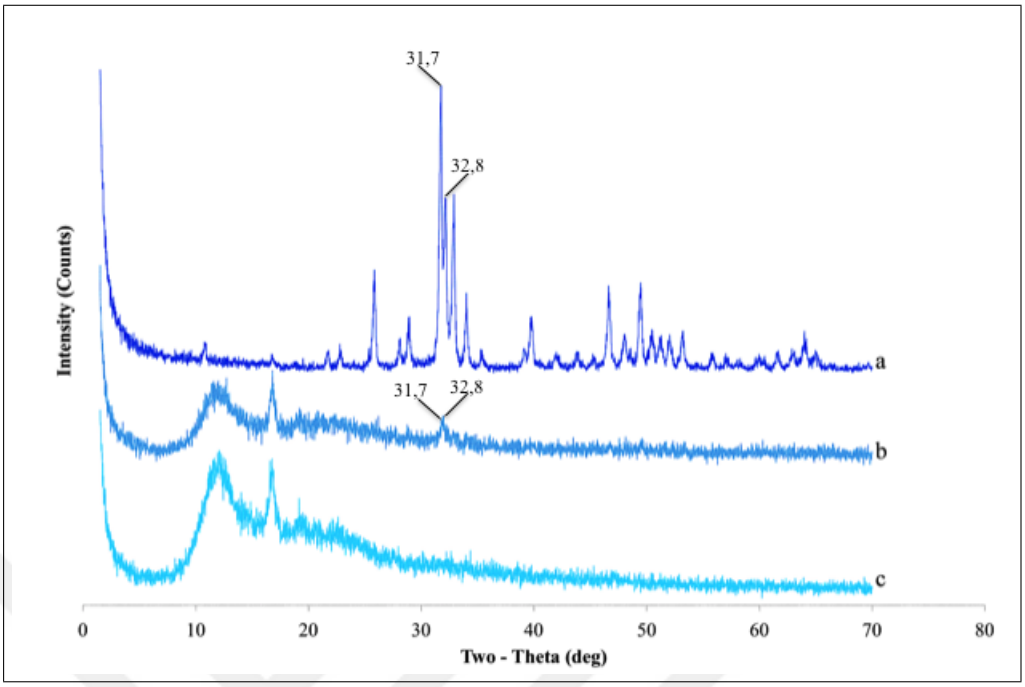

Figure 4.5 XRD patterns of pure HA powder, HA modified PLA scaffolds and unmodified PLA scaffolds. a) HA; b) HA Modified Plain PLA; c) Unmodified Plain PLA.

4.1.4 X-Ray Photoelectron Spectroscopy (XPS)

The surface chemical compositions of Plain PLA and Col-I modified PLA scaffolds were assessed by XPS analysis and the results were given at Figure 4.6 and 4.7. XPS spectra revealed that the C1s and O1s peaks of Plain PLA and Col-I modified PLA scaffolds were very similar to each other. The C1s spectra exhibited peaks at 284.8 eV, 287.1 eV, and 289.3 eV which corresponds to C-C or C-H, C-O, -CO-O respectively [97, 98]. O1s peak was adjusted using one component at 531.8 eV associated to O=C-N [99].

In addition, even though there wasn't any N1s peaks in the XPS analysis result of the unmodified PLA scaffolds; Col-I modified PLA scaffolds has distinctive N1s peaks at 402 and 399 eV which confirms the success of Col-I modification on our scaffolds [100].

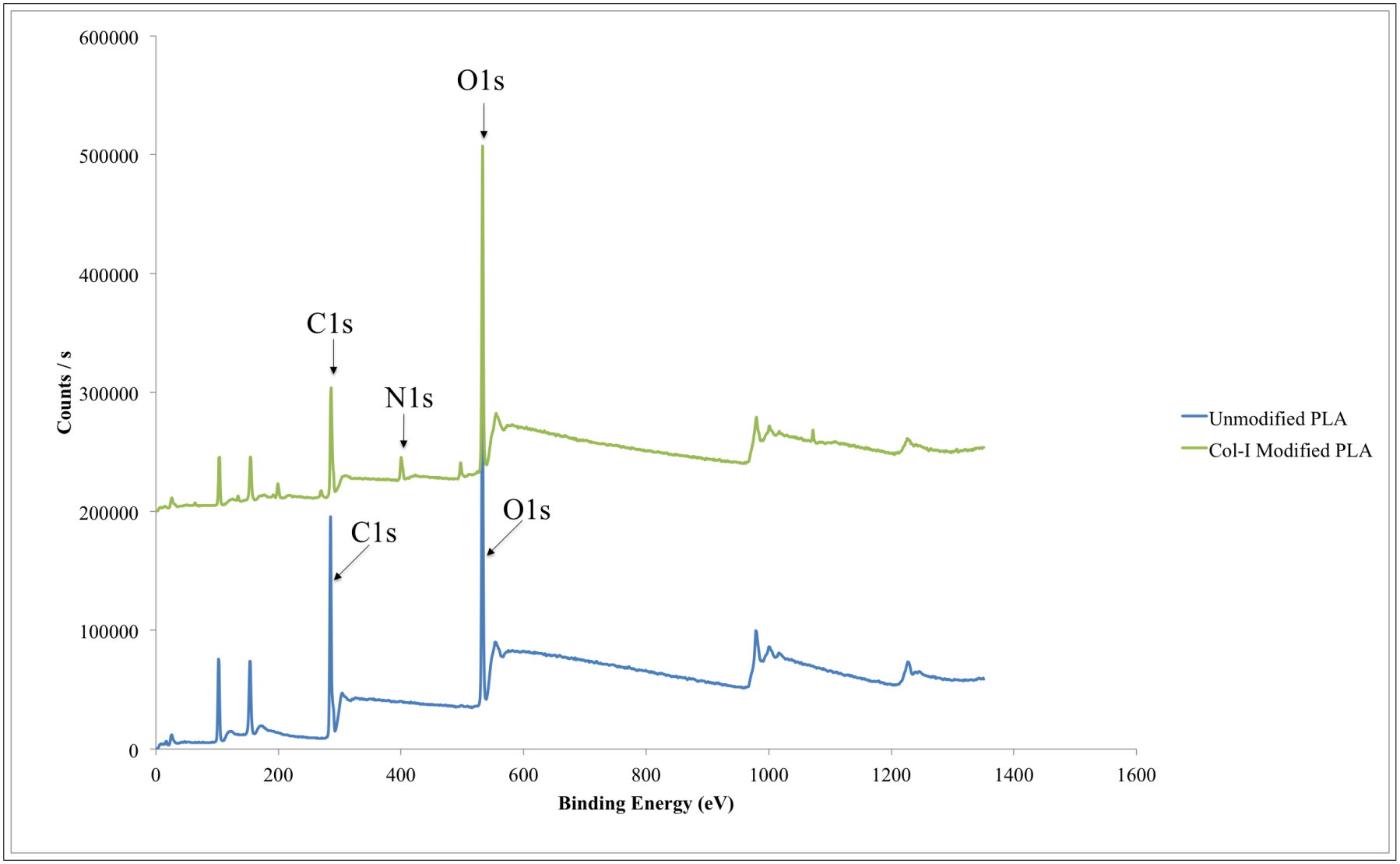

Figure 4.6 XPS spectra of a) Plain PLA and; b) Col-I Modified PLA.

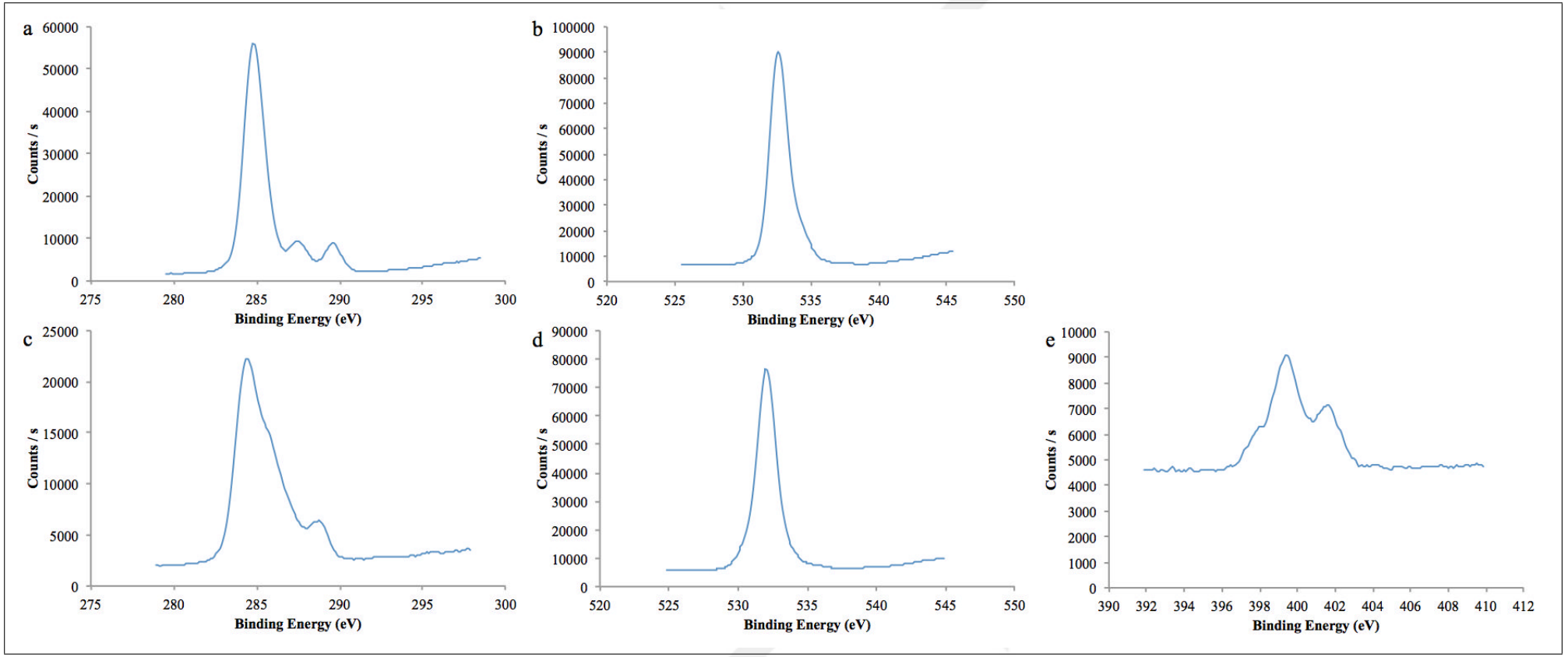

Figure 4.7 C1s, O1s and N1s spectra of the unmodified and Col-I Modified Scaffolds. a) C1s spectra of Plain PLA; b) O1s spectra of Plain PLA; c) C1s spectra of Col-I modified PLA; d) O1s spectra of Col-I modified PLA; and e) N1s spectra of Col-I modified PLA.

4.1.5 Fourier Transform Infrared Spectroscopy (FTIR) Analysis

In order to gain additional information on the chemical structure of the substrate and the immobilization, FTIR spectroscopy was used. The FTIR spectra of a collagen having the molecular formula $C_2H_5NOC_5H_9NOC_5H_{10}NO_2$, PLA having the molecular formula $(C_3H_4O_2)_n$ and HA having the molecular formula $Ca_5(PO_4)_3(OH)$ were given in Figure 4.8.

The IR spectra of modified and unmodified PLA scaffolds exhibited distinctive peaks at 1751 cm^{-1}which corresponds to -C = O ester group and the peaks at 2998, 2947 were assigned to the stretching vibration of -CH2 [101]. In IR spectra of the HA modified scaffolds, characteristic ${PO_4}^{3-}$ peaks were observed. These characteristic bands were existed at 1040 cm^{-1} and 1093 cm^{-1}, which arises from u3 ${PO_4}^{3-}$ and stretching mode of ${PO_4}^{-3}$ group, respectively [102]. In IR spectra of the Col-I modified scaffolds, the amide peak was observed between 1630 and 1655 cm^{-1}, corresponding to N-H bending of the both secondary and primary amides, [103–105]. Hence, it concluded that be said that the HA and Col-I modification on the scaffolds were confirmed by this data.

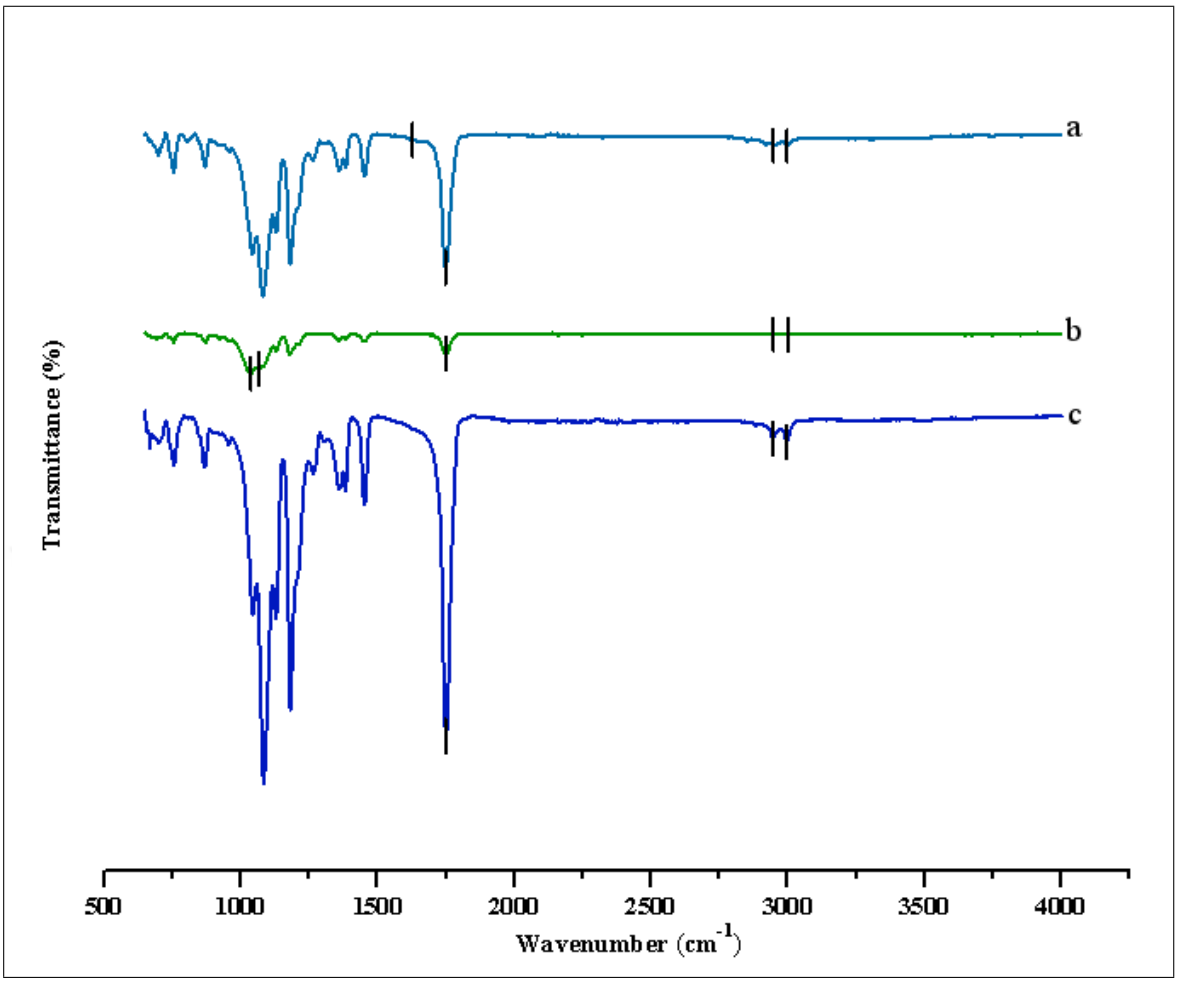

Figure 4.8 The ATR-FTIR spectra of modified and unmodified Plain PLA, a) Col-I Modified Plain PLA; b) HA Modified Plain PLA; c) Unmodified Plain PLA.

4.1.6 In-Vitro BMP-2 Release Profile Analysis

The cumulative BMP-2 release of the Plain and BSM PLA scaffolds were given at Figure 4.9. It was clear that there was a burst effect at first day but after that there was a slight release of the BMP-2. After 4 weeks, Plain and BSM PLA scaffolds released almost the same amount of BMP-2. The cumulative BMP-2 release of the Plain and BSM PLA scaffolds were %99.63 and %100 respectively. According to this data, it concluded that the surface roughness had not any effect on the BMP-2 release of the PLA scaffolds.

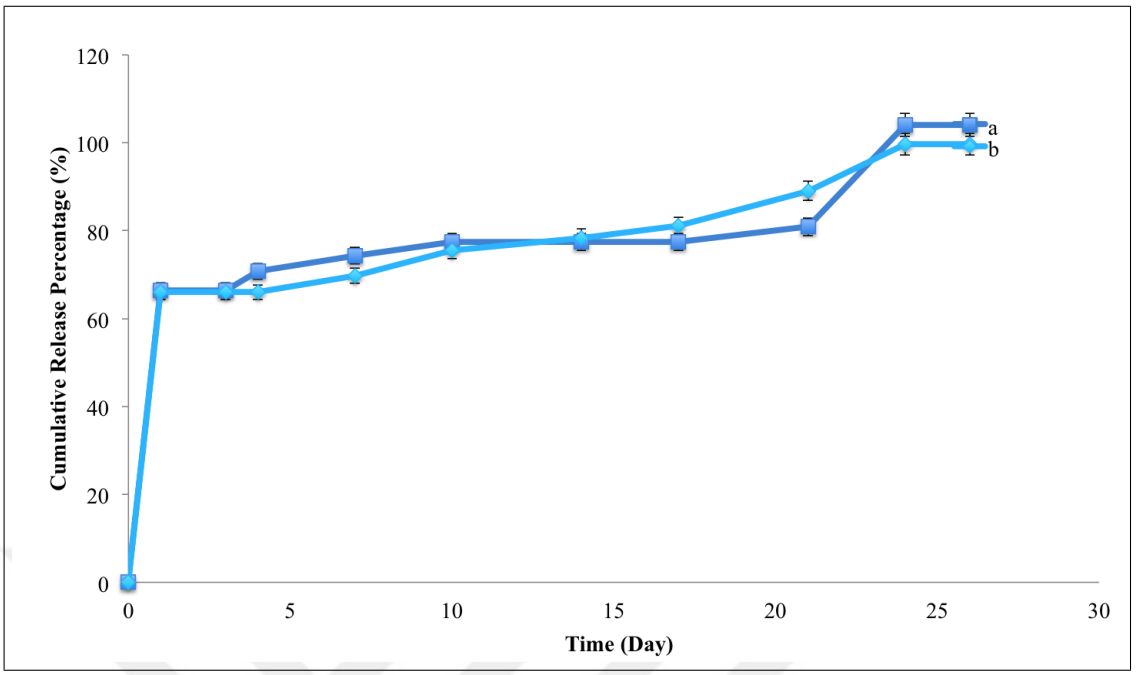

Figure 4.9 The cumulative BMP-2 Release of the Plain and BSM Scaffolds, a) BSM PLA; b) Plain PLA.

4.1.7 Atomic Force Microscopy (AFM) Measurements

The surface properties of the unmodified plain, BSM, Col-I modified BSM and HA modified BSM scaffolds were investigated by using AFM analysis and the results were given at Figure 4.10 and Table 4.2. According to the AFM images, the plain PLA scaffolds had a smooth surface whereas the BSM PLA scaffolds have possed a rough surface. Roughness value of plain PLA is 0.36 ± 0.01 nm. BSM PLA has smooth and rough region whose roughness were 27.14±4.29 nm and 73.07±1.81 nm, respectively. In addition, after the Col-I and HA modifications were performed, the surface roughness of the modified scaffolds was increased. The roughness of the Col-I modified scaffolds was 249.68v18.82 nm and the roughness of the HA modified scaffolds was 95.94 ± 6.02 nm. The increase in the roughness of the Col-I modified scaffolds might be caused by the Col-I immobilization process and the increase in the roughness of the HA modified scaffolds could be due to the non-uniform distribution of the HA on the surface.

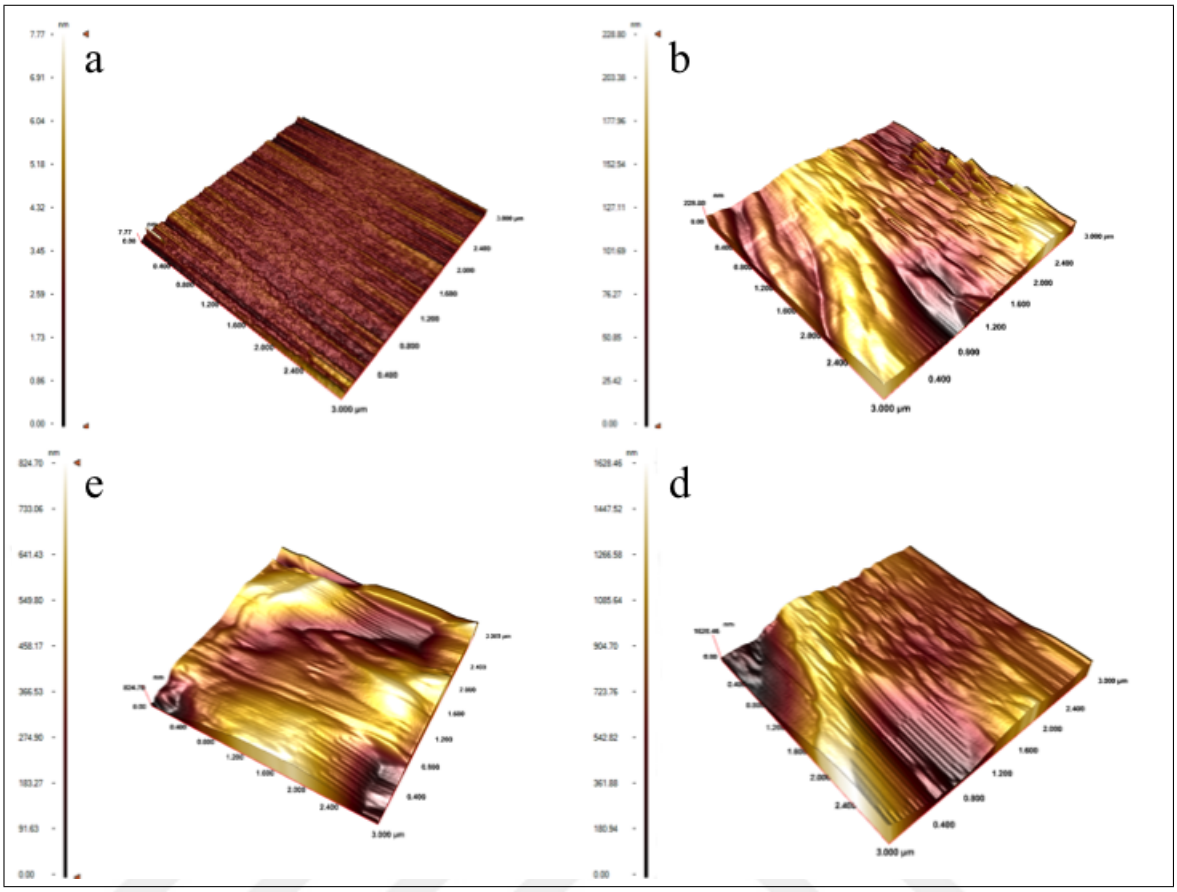

Figure 4.10 The cumulative BMP-2 Release of the Plain and BSM Scaffolds, a) BSM PLA; b) Plain PLA.

Table 4.2
Roughness Measurements Of Unmodified Plain PLA Scaffolds, Unmodified and Modified BSM PLA Scaffolds.

Samples	Roughness (nm)
Plain PLA	0.36±0.01
BSM PLA Smooth Region	27.14±4.29
BSM PLA Rough Region	73.07±1.81
HA Modified BSM PLA	95.94± 6.02
Col-I Modified BSM PLA	249.68±18.82

4.2 Cell Culture Studies

4.2.1 Viability Analysis

The viability percentages of the ADMSC on the modified and unmodified PLA scaffolds were analyzed regarding six different categories by using MTT test. The results were given at Figure 4.11. According to MTT assay of pure PLA scaffolds, after 28 days, there were more viable cells than the first day of the culture. In addition, there was not any significant difference of OD values were found on all scaffolds when the all days were considered. It meant that HA, Col-I and BMP-2 loading provided a suitable surface for cell attachment and proliferation [106]. After Day 4, due to the differentiation of ADMSC, the viability percentage did not increase, which means that during differentiation period, the cells do not divide [107]. Also, this data were consistent to the literature. At day 1, there was a significant increase in the viability of BMP-2 loaded and HA modified Plain and BSM PLA scaffolds. At day 7, there was a significant decrease in BMP-2 loaded and BMP-2 loaded/Col-I Modified scaffolds. In addition, there was a significant increase in the viability of BMP-2 loaded and Col-I modified Plain and BSM PLA scaffolds. At day 14, only the viability of the BMP-2 loaded/HA modified BSM PLA scaffolds was significantly higher than the others. At day 28, there was a significant decrease on the all of the modified scaffolds except the BMP-2 loaded/Col-I modified scaffolds.

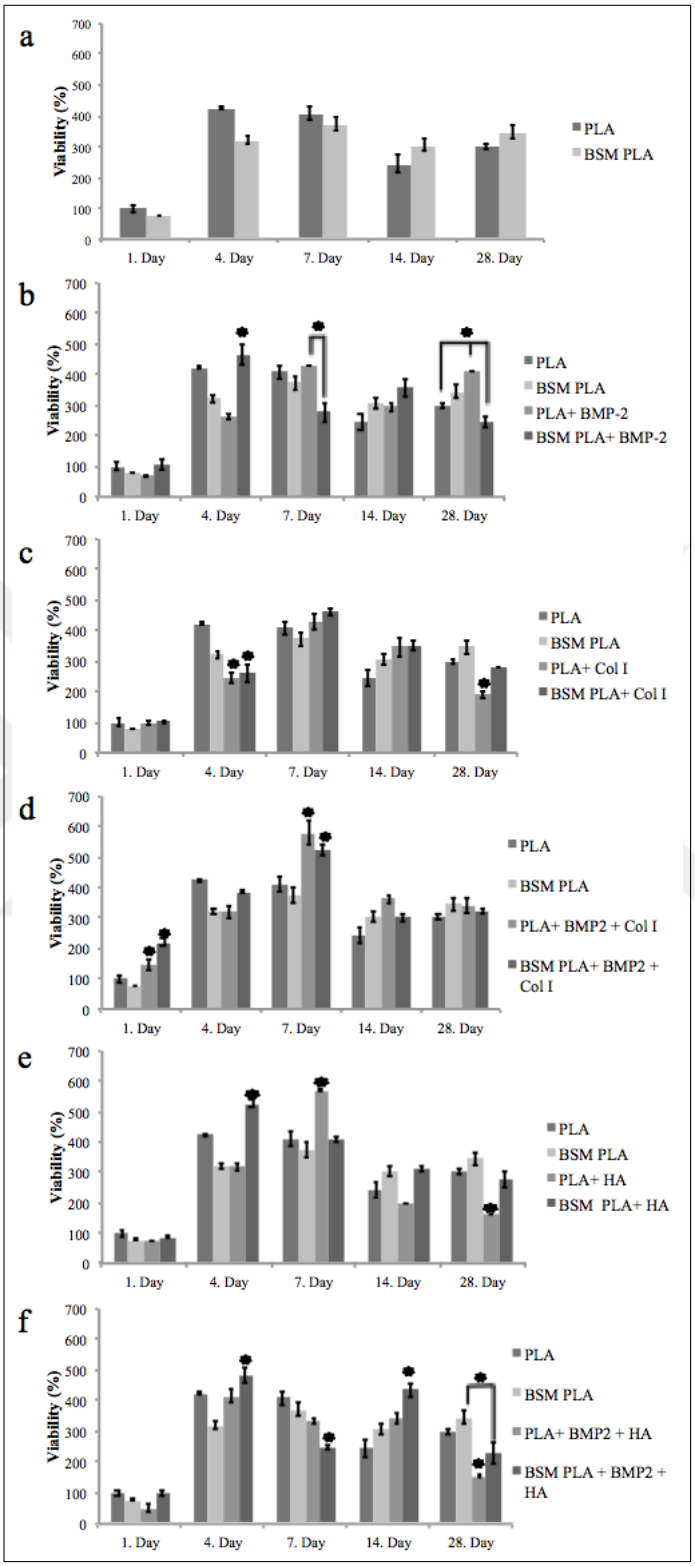

Figure 4.11 The viability of the ADMSC on the scaffolds. The effect of a) surface chemistry b) BMP-2 loading c) Col-I Modification d) BMP-2 loading/Col-I modification e) HA modification f) BMP-2 loading/HA modification.

4.2.2 Proliferation Analysis

The proliferation percentages of the ADMSC on the modified and unmodified PLA scaffolds were analyzed regarding six different categories by using Alamar Blue test. The results were given at Figure 4.12. From day 1 to day 4, there was a significant increase on the proliferation of the ADMSC on the modified and unmodified PLA scaffolds. After day 4, there wasn not any significant increase, which is consistent to the literature because the cells that becomes differentiate would stop their dividing activity [107]. In addition, there was a significant increase in the proliferation of the BMP-2 loaded BSM PLA scaffolds at day 1, HA modified scaffolds and BMP-2 loaded/Col-I modified BSM PLA scaffolds at day 4. At day 7, Col-I modified PLA scaffolds showed the highest proliferation rate while BMP-2 loaded/HA modified scaffolds showed the lowest proliferation percentage. Finally, all of the modified scaffolds except BMP-2 loaded/HA modified ones showed better proliferation than unmodified PLA scaffolds.

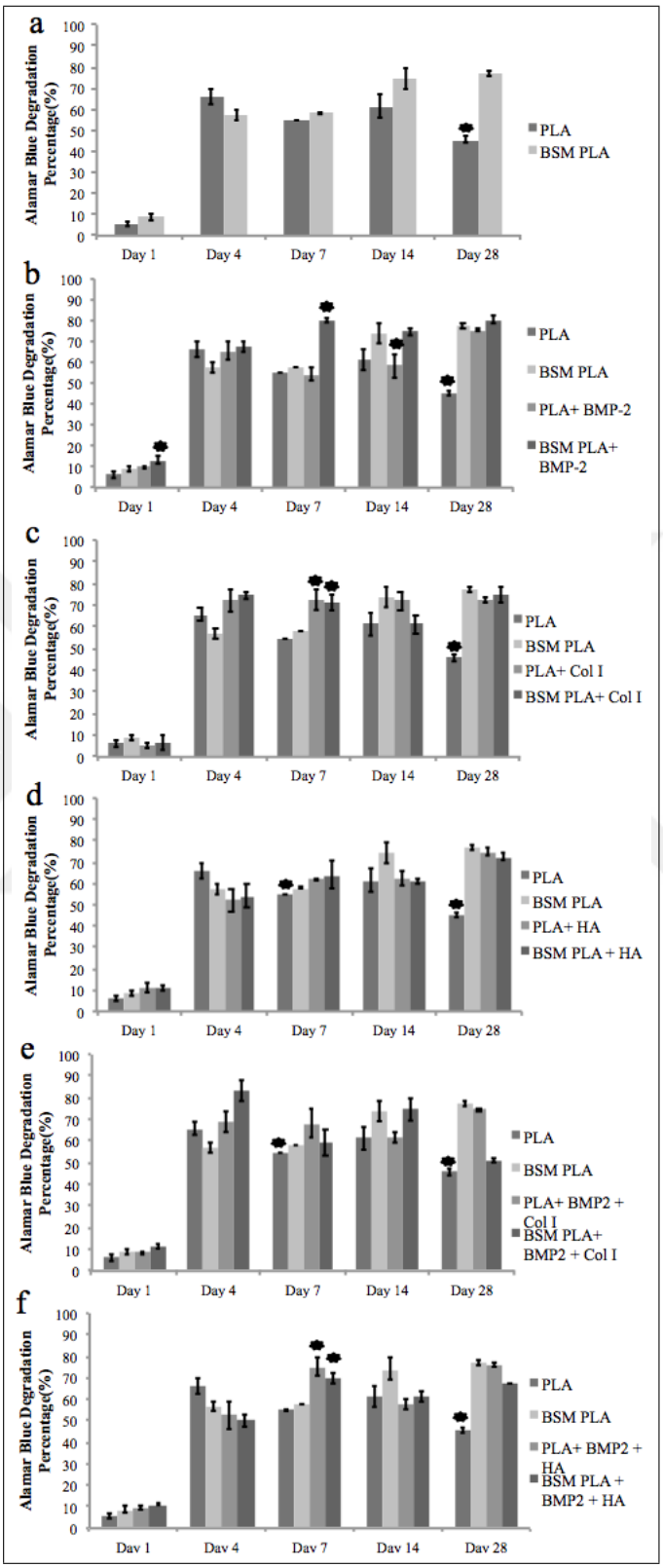

Figure 4.12 The proliferation of the ADMSC on the scaffolds. The effect of a) surface chemistry b) BMP-2 loading c) Col-I modification d) HA modification e) BMP-2 loading/Col-I modification f) BMP-2 loading/HA modification.

4.2.3 Alizarin Red Analysis

In order to analyze the differentiation of the ADMSC on the produced scaffolds, the Alizarin Red Analysis was performed and the results were given at Figure 4.13. to Figure 4.18. In that analysis, with the increase in the Calcium amount, the reddish color of the scaffolds would increase [108]. According to our results, on increasing incubation time, the scaffolds became more reddish. In addition, the colors of the modified scaffolds were more reddish than unmodified scaffolds, which demonstrated that modifications improve the differentiation activity of the ADMSC. Finally, the differentiation activity of the BMP-2 loaded/HA modified and BMP-2 loaded and Col-I modified scaffolds were higher than the others which showed that the BMP-2 loaded/HA modified and BMP-2 loaded/Col-I modified scaffolds were the best group regarding to the differentiation activity of the ADMSC.

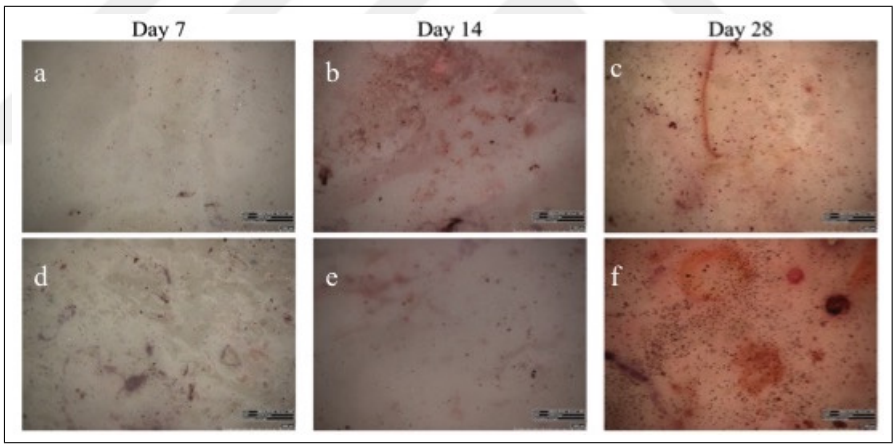

Figure 4.13 The effect of surface topography. Plain PLA scaffolds a) day 7, b) day 14 c) day 21; BSM PLA scaffolds d) day 7 e) day 14 f) day 21

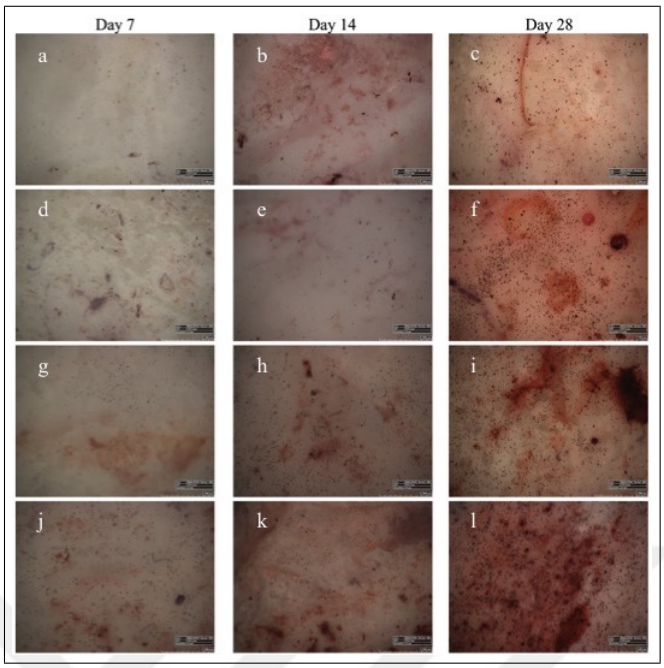

Figure 4.14 The effect of Col-I modification. Plain PLA scaffolds a) day 7, b) day 14 c) day 21; BSM PLA scaffolds d) day 7 e) day 14 f) day 21; Col-I Modified Plain PLA scaffolds g) day 7, h) day 14, i) day 21; Col-I Modified BSM PLA scaffolds j) day 7, k) day 14, l) day 21.

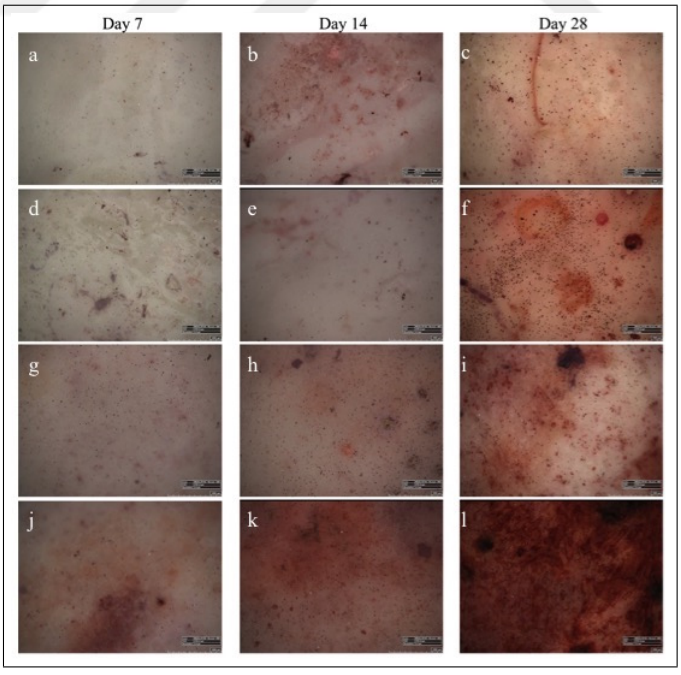

Figure 4.15 The effect of HA modification. Plain PLA scaffolds a) day 7, b) day 14 c) day 21; BSM PLA scaffolds d) day 7 e) day 14 f) day 21; HA Modified Plain PLA scaffolds g) day 7, h) day 14, i) day 21; HA Modified BSM PLA scaffolds j) day 7, k) day 14, l) day 21.

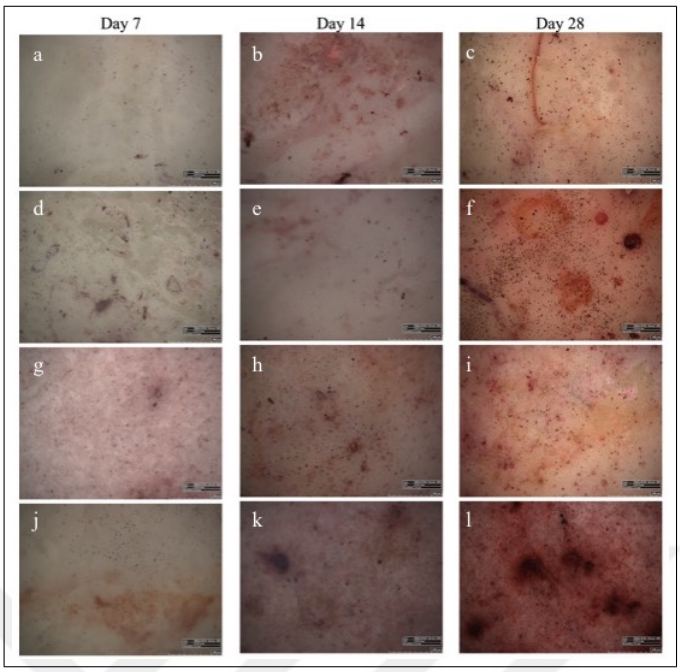

Figure 4.16 The effect of BMP-2 loading. Plain PLA scaffolds a) day 7, b) day 14 c) day 21; BSM PLA scaffolds d) day 7 e) day 14 f) day 21; BMP-2 loaded Plain PLA scaffolds g) day 7, h) day 14, i) day 21; BMP-2 loaded BSM PLA scaffolds j) day 7, k) day 14, l) day 21.

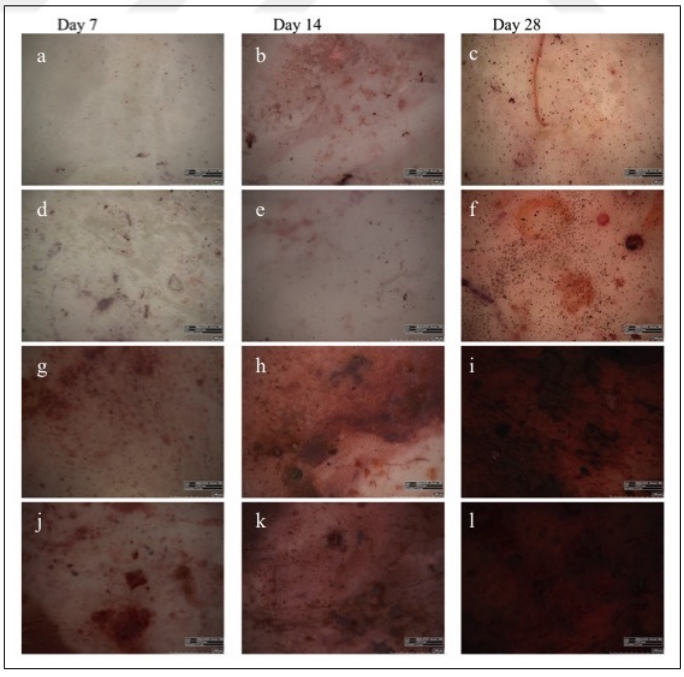

Figure 4.17 The effect of BMP-2 loading/Col-I modification. Plain PLA Scaffolds a) day 7, b) day 14 c) day 21; BSM PLA scaffolds d) day 7 e) day 14 f) day 21; BMP-2 loaded and Col-I Modified Plain PLA scaffolds g) day 7, h) day 14, i) day 21; BMP-2 loaded and Col-I Modified BSM PLA scaffolds j) day 7, k) day 14, l) day 21.

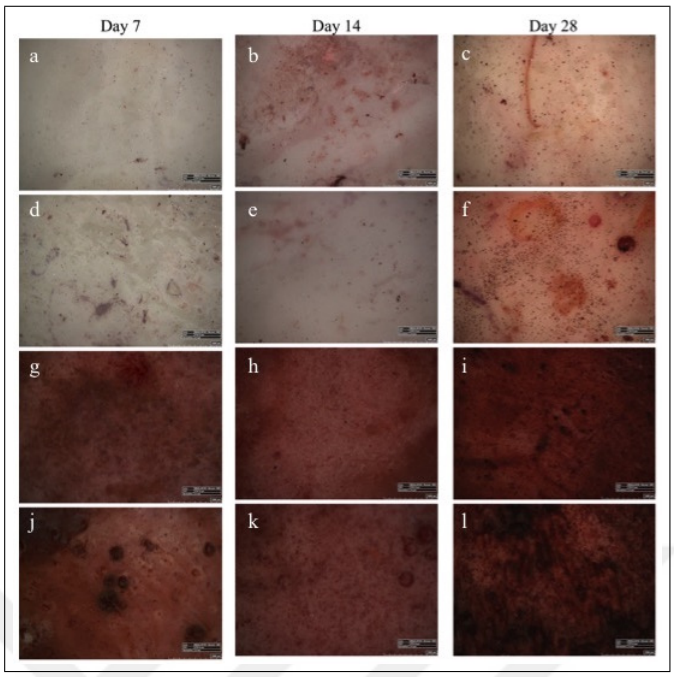

Figure 4.18 The effect of BMP-2 loading/HA modification. Plain PLA scaffolds a) day 7, b) day 14 c) day 21; BSM PLA scaffolds d) day 7 e) day 14 f) day 21; BMP-2 loaded and HA modified Plain PLA Scaffolds g) day 7, h) day 14, i) day 21; BMP-2 loaded and HA modified BSM PLA scaffolds j) day 7, k) day 14, l) day 21.

4.2.4 ALP Analysis

In order to investigate the difference of the osteogenic differentiation of the ADMSC, ALP analysis was performed because with the increase of the alkaline phosphatase activity of the cells, the differentiation mechanism started. The results of this analysis were given at Figure 4.19. It was expected that, the ALP activity of the cells would increase and that activity would have its highest value at day 14 [107]. According to our results, At day 14, the BMP-2 loaded BSM, Col-I modified BSM, HA modified plain and BSM, BMP-2 loaded/Col-I Modified Plain and BSM amd BMP-2 loaded/HA Modified Plain and BSM Scaffolds were statistically significantly increased. In addition, at day 21, only BMP-2 loaded/Col-I Modified BSM Scaffolds were significantly higher than the others. The ALP activity of the cells rose and that activity had its highest value at day 14, which is consistent to the literature as well.

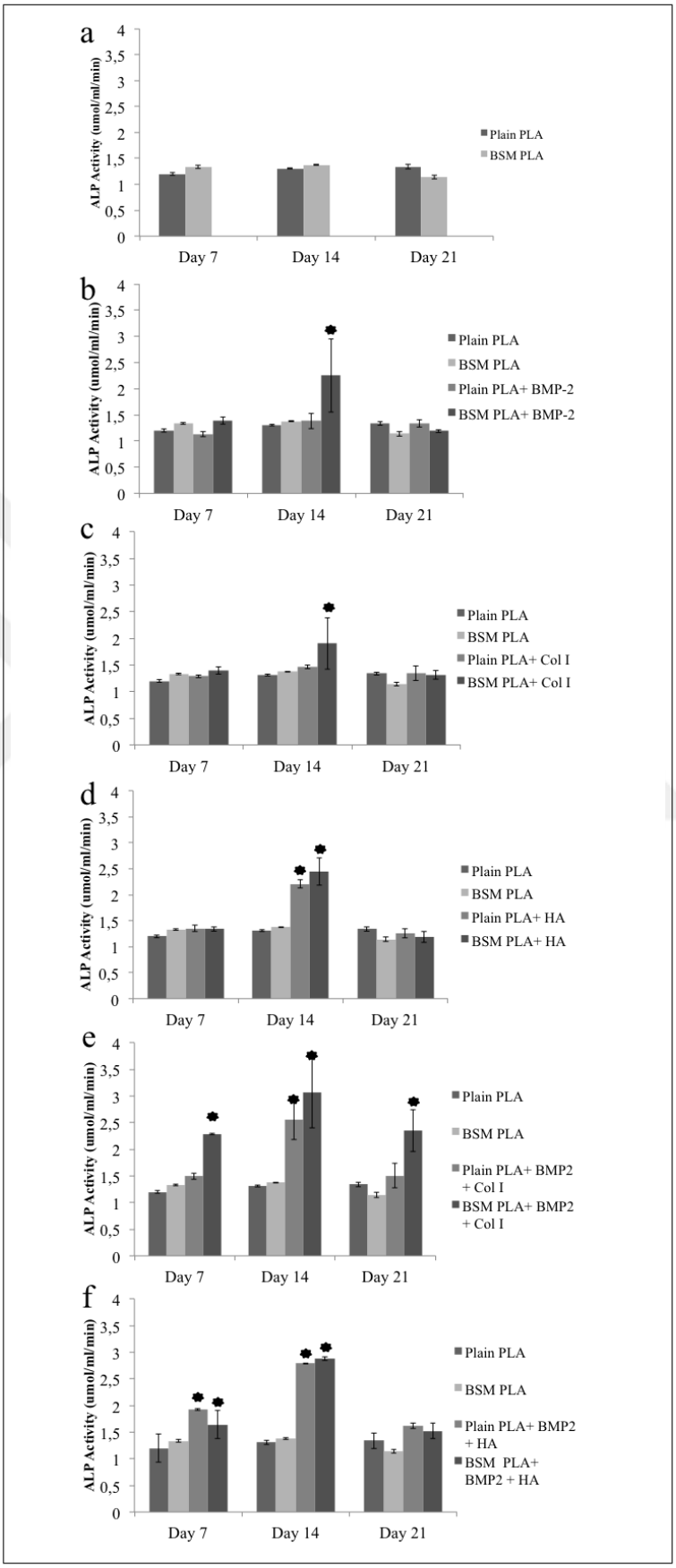

Figure 4.19 ALP activity of the ADMSC on the scaffolds. a) The effect of surface chemistry b) The effect of BMP-2 loading c) The effect of Col-I modification d) The effect of HA modification e) The effect of BMP-2 loading/Col-I modification f) The effect of BMP-2 loading/HA modification.

4.2.5 SEM Analysis

The morphology and the HA deposition of the ADMSC on the modified and unmodified scaffolds were analyzed by SEM EDAX and the SEM images were given at Figure 4.20. According to the SEM images, mineral deposition on the BMP-2 loaded/Col-I modified and BMP-2 loaded /HA modified PLA scaffolds were observed at day 28 [108]. That deposition was also correlated with the EDAX results of these samples, which were given at Table 4.3. Ca/P molar ratios of the BMP-2 loaded/Col-I modified Plain PLA scaffolds, BMP-2 loaded/Col-I modified BSM PLA scaffolds, BMP-2 loaded/HA modified Plain PLA scaffolds, BMP-2 loaded/HA modified BSM PLA scaffolds were 1.33, 1.49, 1.22 and 1.33, respectively. The Ca/P ratio of these surfaces was close to 1.5 of the pure HA component tricalcium phosphate and 1.33 of the HA precursor octacalcium phosphate in vivo [107, 109]. In addition, it might be considered that the high Ca/P molar ratio values might be caused due to HA presence on the BMP-2 loaded/ HA modified scaffolds. However, EDAX measurements of these scaffolds were taken from the area, which looked like cell debris.

Table 4.3
WCA Measurements of Modified and Unmodified Plain And BSM PLA Scaffolds.

Groups	Ca/P Ratio	Reference Values
BMP-2 Loaded/Col-I Modified Plain Scaffolds	1.33	1.5 [109] - 1.33 [107]
BMP-2 Loaded/Col-I Modified BSM Scaffolds	1.49	1.5 [109] - 1.33 [107]
BMP-2 Loaded/HA Modified Plain Scaffolds	1.22	1.5 [109] - 1.33 [107]
BMP-2 Loaded/HA Modified BSM Scaffolds	1.33	1.5 [109] - 1.33 [107]

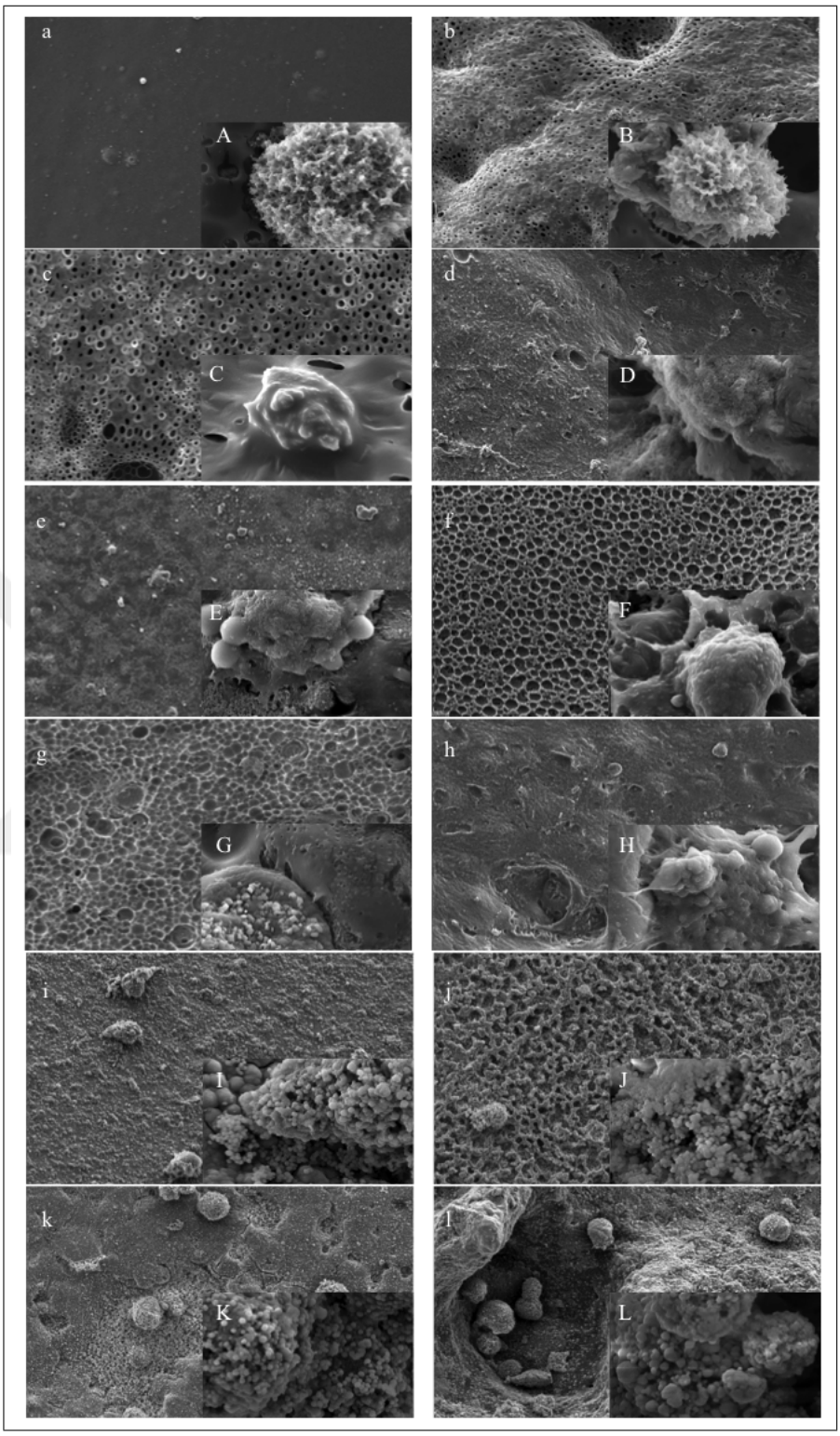

Figure 4.20 SEM images at day 28 with 1000X (inset 10000X) magnification. a) Plain PLA scaffolds; b) BSM PLA scaffolds c) BMP-2 loaded Plain PLA scaffolds; d) BMP-2 loaded BSM PLA scaffolds; e) Col-I modified Plain PLA scaffolds; f) Col-I modified BSM PLA scaffolds; g) HA modified Plain PLA scaffolds; h) HA modified BSM PLA scaffolds; i) BMP-2 loaded/Col-I modified Plain PLA scaffolds; j) BMP-2 loaded/Col-I modified BSM PLA scaffolds; k) BMP-2 loaded/HA modified Plain PLA scaffolds; l) BMP-2 loaded/HA modified BSM PLA scaffolds.

5. DISCUSSION

Materials, which are used in the orthopedic clinical usage, is divided into three generations based on their bio-function by Navarro et al [110]. In the first generation, there would be bio-inert materials' which are used as a filler for the gaps. The second-generation contains composites, which are biodegradable and bioactive materials to cooperate with the biological environment across the fracture for improving the tissue/surface bonding and the biological response. In addition, the second generation materials are bioabsorbable and able to perform progressive degradation during new tissue regeneration and healing such as poly(lactic-co- glycolide) (PLGA) copolymers, PLA and PGA. Finally, the third-generation materials are intended to excite specific cellular responses. These materials have three-dimensional structures, which are biocompatible and biodegradable and their by-products aren not cytotoxic [111].

PLA, which is FDA approved synthetic biodegradable polymer, was firstly reported as bio-absorbable surgical device by Kulkarni et al. [112]. It has various good characteristic features like biodegradability, good biocompatibility, good process ability [112]. HA has been extensively used as an implant for bone regeneration and various biomedical applications, owing to its biodegradable, bioactive and osteoconductive properties. Though, the usage of pure HA particle is limited because of its brittleness. Thereby, Tian et al prepared Poly (L-lactide) (PLLA)/HA composite and they found that PLA/HA composite showed good osteoconductivity and osteoinductivity [113].

According to Tsuji et al., BMP-2 is the high standard of growth factor to regenerate bone [114]. Nonetheless, upholding useful therapeutic concentrations is problematic because of a short half-life in vivo. Several delivery systems have been established for BMP-2 release [115]. Burkus et al. developed collagen based delivery of the BMP-2 [116]. Sawyer et al used tricalcium phosphate to investigate useful delivery mechanism for the BMP-2 [117]. In addition, by Wang et al, the 3D printed porous HA scaffold with embedded BMP-2 was used for bone tissue engineering applications [118, 119].

Generally, bone regeneration has been studied by investigating new scaffolds which mimic 3D structure of the bone [120, 121] or the biochemical composition of it [122]. However, the bone regeneration and modeling arise on the surface of bone [90]. Thereby, the morphology of the bone surface is crucial during healing process [91]. Rather than investigating new 3D structure or chemical composition mimicked scaffolds, previous studies also proved that it is possible to mimic bone surface topography microenvironment by using bone itself [76]. Nevertheless, mimicking only the surface topography of the bone could not be enough to mimic bone microenvironment. To the best of our knowledge, there has been no study, which aimed to understand the synergetic effect of the surface topography of the bone and its biochemical structure mimic. From that point, in this thesis, comprehending the synergetic effect of the surface topography of the bone and its biochemical structure mimic is aimed.

In order to understand the effectiveness of the BSM mimicking and the success of the HA and Col-I modifications, the surface properties of the scaffolds were analyzed with SEM, WCA and AFM. In addition, the chemical compositions of the modified and unmodified PLA scaffolds were examined by FTIR, XRD and XPS. Growth factor release profile of PLA scaffolds were also studied. Finally, the characterization studies were followed by the cell culture studies. The viability, proliferation and osteogenic differentiation of the ADMSC on plain and BSM, modified and unmodified PLA scaffolds had been investigated by using MTT test, Alamar Blue Analysis, Alizarin Red Staining and ALP analysis, respectively.

The surface properties of the Col-I or HA modified or unmodified plain and BSM scaffolds were investigated by using SEM. The surface topography images of the modified and unmodified PLA scaffolds were given in Figure 4.1- Figure 4.3. In SEM analysis, affectivity of the BSM mimicking and the success of the HA and Col-I modifications were analyzed. Firstly, it should be noticed that the BSM scaffolds, which are produced by using PDMS molds, should be able to mimic the surface topography of the bone. According to the SEM images, it could be said that BSM scaffolds were produced successfully because our results were similar to the previous studies (Figure 4.1-Figure 4.3) [76]. Furthermore, the surface morphology of Col-I and HA modified

scaffolds were quietly different than their unmodified versions as it could easily be observed at Figure 4.1-Figure 4.3. HA particles, whose size is 200 nm, were monitored on the surface of the HA modified scaffolds and Col-I, which assembles into fibrils, and has gap regions because of the staggered arrangement, was seen on the surface of the Col-I modified scaffolds [92]. In addition, the morphology of HA particles or Col-I on our modified samples are consistent to the studies of the Kleinheinz et al and Santos et al, which confirmed the success of the HA and Col-I immobilization on the scaffolds [123, 124].

Material surface wettability is a macroscopic effect, which is affected mainly by chemical functionality and topography of the surfaces. Due to the different wettability properties of the surfaces, proteins would adsorb in different ways onto them which effects the adhesion, proliferation and differentiation of different type of cells [124]. In order to estimate the effect of the produced scaffolds on the adhesion, proliferation and differentiation of ADMSC, the wettability of the surfaces was analyzed by performing WCA measurements. WCA measurements were taken from three different contact points of each samples as well as three different samples from each group were used for that measurement process. WCA values of plain PLA and BSM HA or Col-I modified and unmodified PLA scaffolds were given in Table 4.1 and their contact angle images were given in Figure 4.4. Contact angle value of plain PLA was 101.68 $\pm$ 7.68° which is similar with PLA surface of Schaub et al study [125]. According to Ma et al, after collagen type I immobilized on the PLA surface, the WCA was decreased from 71.00$\pm$1,60° to 35.00$\pm$3,40°. The hydrophilic property of the Col-I modified samples was increased twofold which is also similar the results of Ma et al [126]. According to Chen et al. the WCA degree of the HA coated PLA membranes 29.00 $\pm$ 3.00°. The WCA result of the HA modified Plain PLA was 33.39 $\pm$ 5.07° and this result was similar to Chen et al. study. In addition, unmodified BSM PLA scaffolds were more hydrophobic than Plain PLA scaffolds and modified BSM PLA scaffolds were more hydrophilic than modified Plain PLA scaffolds, which could be explained by Wenzel Theorem [127]. According to this theorem, with the increase of the surface roughness, the hydrophobic materials become more hydrophobic and hydrophilic materials become more hydrophilic [127]. According to Ahn et al, the

proliferation of hADSCs on rough and hydrophilic surfaces was higher than that on smooth and hydrophobic and surfaces [93].

In order to check the success of the HA modifications on the plain PLA scaffolds, XRD test was performed. The static XRD Analysis of the Pure HA powder, HA modified or unmodified Plain PLA Scaffolds were given at Figure 4.5. It was expected that HA modified Plain PLA scaffolds would have similar peaks with either, the unmodified Plain PLA scaffolds and Pure HA powder. As it could be seen at Figure 4.5, the diffraction patterns of Pure HA powder and HA modified Plain PLA scaffolds showed two peaks at 31.70 and 32.90, which are the main reflection planes of apatite-like calcium phosphate according to Abdal-hay et al. , Deplaine et al. and Tanimoto et al. [95, 96, 128]. In contrast, Plain PLA hadn not any of these characteristic peaks. Thus, it could be said that the HA modification of the PLA surfaces was successful.

After Col-I modification of the PLA scaffolds, the surface chemical composition changes on the modified scaffolds were analyzed by XPS analysis and the results were given at Figure 4.6 and 4.7. PLA having the molecular formula (C3H4O2)n has Carbon and Nitrogen atoms in its structure. Thereby, it was expected that C1s spectra and O1s spectra of the Col-I modified and unmodified PLA scaffolds exhibited the same peaks. The C1s peak was adjusted using three peaks 284.8 eV, 287.1 eV, and 289.3 eV corresponding to C-C or C-H, C-O, -CO-O respectively [97, 98]. The O1s spectra exhibited peaks at 531.8 eV associated to O=C-N [99].

According to Cui et al. , the peaks between 402 and 399 eV are the characteristic nitrogen peaks [100]. The unmodified PLA, having the molecular formula $(C_3H_4O_2)n$, has not got any nitrogen atom its structure unlike the Col-I modified PLA, which has collagen, having molecular formula $C_2H_5NOC_5H_9NOC_5H_{10}NO_2$, in its structure. Thereby, the presence of the nitrogen could be able to prove the success of our Col-I modification. As it was expected, Col-I modified PLA scaffolds was enriched with nitrogen atoms, which presented similar binding energies to pure collagen, because these scaffolds had a characteristic N1s peak between 402 and 399 eV. In contrast there wasn not any N1s peak in the XPS spectrum of the unmodified PLA scaffolds, which

confirmed that these scaffolds had not got nitrogen atom in its structure. Thereby, it could be said that Col-I modification on our scaffolds was achieved.

With the Col-I and HA modifications of the PLA scaffolds, the surface chemical composition on the modified scaffolds were changed and the change of the composition was analyzed by FTIR analysis. The FTIR spectra of a collagen that have the molecular formula $C_2H_5NOC_5H_9NOC_5H_{10}NO_2$, PLA, which have the molecular formula $(C_3H_4O_2)n$ and HA, which have the molecular formula $Ca_5(PO_4)_3(OH)$ were given in Figure 4.8.

According to Hoidy et al., the IR spectra of the PLA exhibited distinctive peaks at 1751 cm^{-1} corresponding to -C = O ester group and the peaks at 2998 and 2947 cm^{-1} were assigned to the stretching vibration of -CH_2 bonds [101]. As it was expected, modified and unmodified PLA scaffolds showed all of these distinctive peaks in their IR spectra.

In addition, it was also expected that there should be characteristic ${PO_3}^{3-}$ peaks in the IR spectra of HA modified scaffolds and Amide peaks in the IR spectra of Col-I modified scaffolds. As it was expected, the band at 1040 cm^{-1} arises from $\upsilon 3$ ${PO_3}^{3-}$ as well as the bands at 1093 cm^{-1} arises from stretching mode of ${PO_4}^{3-}$ group [102] in the data of the HA modified scaffolds and the amide peak was existed between 1630 and 1655 cm^{-1}, corresponding to N-H bending of the both secondary and primary amides, in the data of the Col-I modified scaffolds [103–105]. In contrast, there wasn not any characteristic PO3 and Amide peaks in the IR spectra of the unmodified PLA scaffolds. Therefore, HA and Col-I modification on the PLA scaffolds were confirmed with this data.

In order to see the effect of the surface topography on the BMP-2 growth factor release, the cumulative BMP-2 release of the Plain and BSM PLA scaffolds were analyzed and the results were given at Figure 4.9. To begin with, the release profile of BMP-2 from plain PLA is consistent to the study of the Faßbender et al. [80]. According to the results, there was a burst effect at first day but after that there was a slight

release of the BMP-2, as expected.

In addition, if the surface topography has an effect on the BMP-2 release from the surfaces, an increase of the surface roughness would cause a rise in the BMP-2 release from the scaffolds because of the increase in surface area of the scaffolds. However, there wasn not any significant difference between the cumulative BMP-2 release of the Plain and BSM PLA scaffolds. According to this data, it could be said that the surface roughness hadn not any effect on the BMP-2 release profile of the PLA scaffolds. It was also consistent with the literature because Yilgor et al. showed that BMP-2 release profile is not regarding to the architecture of the scaffolds it only relates to the chemical composition of the scaffolds [129, 130].

According to Wennerberg et al. [91], the surface roughnesses of the scaffolds are crucial factors for the attachment of the cells [91]. The rough surfaces possess more advantageous than the smooth surfaces in cell studies [91]. In order to estimate the cell behaviors on the produced modified scaffolds, the surface roughness of the Col-I or HA modified or nonmodified plain and BSM scaffolds were investigated by using AFM analysis and the results were given at Figure 4.4 and Table 4.1. The roughness values of the BSM PLA scaffolds (Ra: 27.14±4.29/73.07±1.81) were higher than plain PLA scaffolds (Ra: 0.36±0.01 nm). In addition, the BSM PLA scaffolds has either, rough and smooth regions. According to the Palin et al. studies, due to the high roughness value of the bone surface, in nano scale, it does not have homogenous roughness [131, 132]. Thereby, the AFM results of the Plain and BSM scaffolds were consistent to the literature. According to Más, Bruna Antunes, et al, collagen has net-like fibrillar structure. Thus, it was expected that Col-I deposition on the surface promotes an increase in the roughness [99]. The the roughness of the Col-I modified BSM membranes (Ra: 249.68±18.82 nm) were higher than the roughness of nonmodified BSM membranes which confirm that the success of the collagen immobilization on the scaffolds. According to Bottino et al, HA has overall bamboo-like fiber appearance. Thereby, it was expected that expected that HA deposition on the surface endorses a rise in the roughness [133]. When the roughness of the HA modified BSM PLA scaffolds compared with the unmodified scaffolds, HA modification caused formation of rougher

surfaces (Ra = 95.94±6.02 nm), as can be seen in both the SEM (Figure 4.3) and AFM images (Figure 4.4). These results demonstrate the success of the modifications and were consistent to the literature.

The effect of the surface topography on viability, proliferation and differentiation of the ADMSC was analyzed by using MTT, Alamar Blue, Alizarin Red and SEM analysis respectively. According to these analyses, there was not any significant difference between Plain and BSM PLA scaffolds. Thereby, it was observed that the surface topography of the scaffolds did not have any significant effect on the differentiation and proliferation of the scaffolds and it did not show cytotoxic effects as the plain PLA scaffolds.

The effect of the Col-I Modification on viability, proliferation and differentiation of the ADMSC was examined. According to the Li and Jiashen et al., the Col-I modification is not cytotoxic and it also introduces the osteogenic differentiation of the ADMSC [107]. When MTT results of the each day were considered, Col-I modifications on the surfaces did not have any cytotoxic effect on the ADMSC. According to Alamar Blue analysis, the Col-I modification improves the proliferation of the ADMSC at day 7 and day 28. In addition, according to the ALP and Alizarin Red analysis, Col-I modified Plain and BSM scaffolds showed higher osteogenic differentiation activity, which is consistent to the Li and Jiashen et al. study. In addition, According to the ALP data, Col-I modification and BSM has a synergistic effect on the differentiation of ADMSC.

The effect of the HA Modification on viability, proliferation and differentiation of the ADMSC was studied. According to Lv, Qing, et al and Rizzi, Simone C., et al., HA is a not cytotoxic effect on the mesencymal stem cells and it helps the initiation of ADMSC's osteogenic differentiation [134, 135]. According to MTT results, HA modified PLA scaffolds were not cytotoxic and from the Alamar Blue data, it could be concluded that HA modification did not have any negative effect on the proliferation of the ADMSC. Additionally, ALP analysis demonstrated that the HA modification of the scaffolds improves osteogenesis. The Alizarin Red analysis of these scaffolds also

confirms the results of the ALP analysis and the results of Alizarin Red analysis showed that a synergistic effect occurs with BSM and HA modification. To the best of our knowledge, there has been no study which had been tried to investigate the synergistic effect of BSM and HA modification on the osteogenesis.

The effect of the BMP-2 loading on viability, proliferation and differentiation of the ADMSC was investigated. According to Schofer and Markus D. et al., BMP-2 loaded scaffolds were not cytotoxic and they also differentiate [115]. In addition, Ji and Ye, et al suggested that BMP-2 loaded scaffolds had higher osteogenic capacity [136]. Based on MTT results, it could be concluded that BMP-2 release from the scaffolds was not cytotoxic and regarding to the Alamar Blue analysis, BMP-2 release from the scaffolds didn?t cause any significant change in the proliferation of the ADMSC which is consistent to the literature. In addition, the cells on the BMP-2 loaded BSM scaffolds showed better osteogenesis than the cells on the other groups, which could be also the synergistic effect of BSM and BMP-2 load on the osteogenesis of the ADMSC.

The effect of the BMP-2 loading /HA Modification on viability, proliferation and differentiation of the ADMSC was investigated. Cui et al. studied on the BMP-2 loaded HA modified PLGA scaffolds and they suggest that these scaffolds would be accepted as a secure and histocompatible for bone tissue engineering applications. When the MTT data of the day 4, 7, 14, and 28 and Alamar Blue results of the day 4, 7, 14 and considered, the cells on the unmodified scaffolds showed better viability and proliferation activity. Additionally, regarding to the Alizarin Red and SEM analysis, the cells on BMP-2 loaded HA modified PLA scaffolds showed high osteogenesis. Finally based on the SEM and Alizarin Red results, the osteogenic differentiation of the ADMSC on the BMP-2 loaded HA modified BSM PLA scaffolds were higher than BMP-2 loaded HA modified Plain PLA scaffolds. Thereby, the cells on the BMP-2 loaded HA modified PLA scaffolds had demonstrated higher osteogenic activity and the bone surface topography mimicking further enhanced that activity as well.

The effect of the BMP-2 loading/Col-I Modification on viability, proliferation and differentiation of the ADMSC was analyzed. Based on the studies of Ji et al,

it could be said that Col-I on the surfaces delayed the release of the BMP-2, which improves osteogenesis [136]. According to our MTT and Alamar Blue results, BMP-2 Loaded and Col-I Modified scaffolds improved viability and proliferation of the ADMSC. In addition, regarding to the Alizarin Red and ALP data, these scaffolds enhances the osteogenic differentiation of the ADMSC. In addition, the SEM and ALP results demonstrated that BMP-2 Loaded and Col-I Modified BSM scaffolds has higher osteogenic differentiation capacity than BMP-2 Loaded and Col-I Modified plain scaffolds which also confirms that the surface topography and the biochemical property of the material has an effect on osteogenic differentiation.

To sum up, based on the characterization studies, the Col-I/HA modification of the surfaces was successful and the BMP-2 release from the scaffolds were consistent to the literature. In addition, regarding the cell culture studies, BMP-2 loaded/Col-I Modified as well as BMP-2 loaded/HA Modified membranes were the best groups regarding to the differentiation of the ADMSC. It might be caused the synergistic effect of the usage of BMP-2 and HA as well as BMP-2 and Col-I together. In addition, the cells on BMP-2 loaded/Col-I Modified scaffolds showed better proliferation and viability. Thereby, BMP-2 loaded/Col-I Modified scaffolds were found to be the best groups in this study.

5.1 Future Studies

The findings of this thesis may be advantageous to apprehend the changing the characteristics of scaffolds like its surface roughness and topography, chemical and biochemical content, had an effect on cell-surface, cell-tissue scaffold interface characteristics as well as behavior and mechanism of the cells.

In order to analyze the differentiation of the ADMC on the modified and unmodified PLA scaffolds further, immunohistochemistry and gene expression analysis will be done. In addition, to identify the morphology and the attachment of the cells on the modified and unmodified PLA scaffolds, Alexa Flour Analysis will be performed.

After that, all of the experiments will be repeated by using non-osteogenic medium to examine the effect of the medium on the osteogenic differentiation of the ADMSC. Finally, for examining these cell behavior in a real-time, bioreactor might be used to examine the cell behaviors on the best scaffolds, which initiated better cell viability, proliferation and differentiation behavior, as a the future aspects.

APPENDIX A. CALIBRATION CURVE

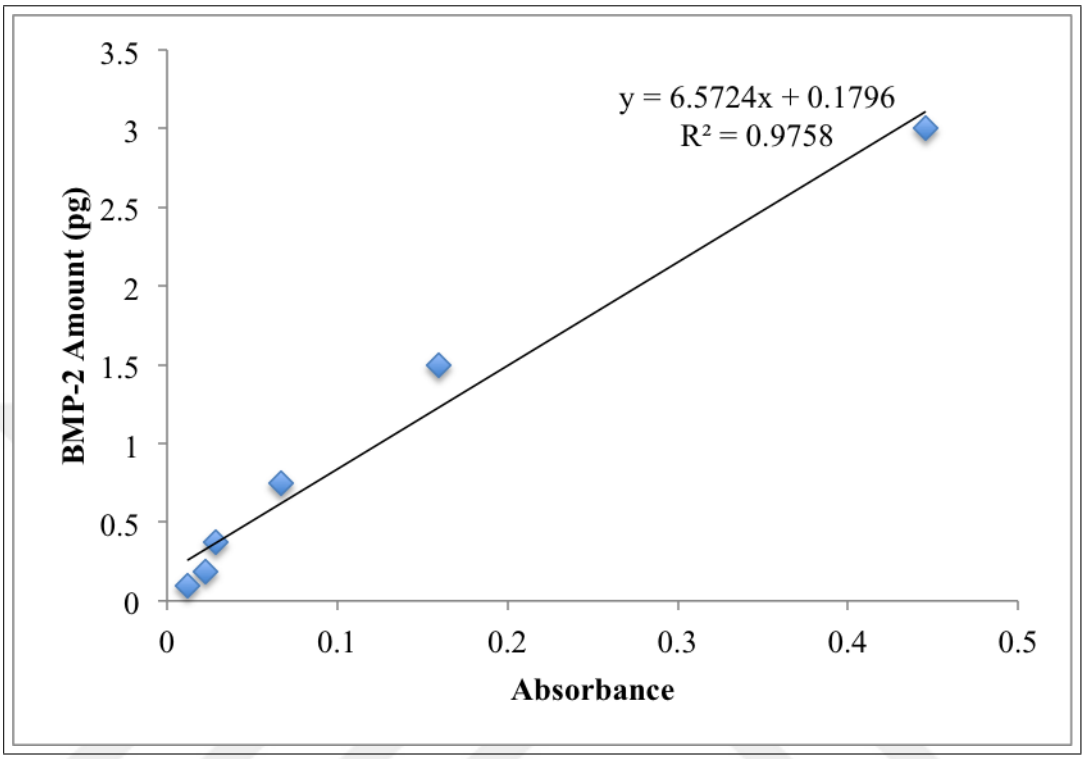

Figure A.1 MP-2 calibration curve at 276 nm.

REFERENCES

1. Hwang, J., Y. Jeong, J. M. Park, K. H. Lee, and J. W. Hong, "Biomimetics : forecasting the future of science , engineering , and medicine," pp. 5701–5713, 2015.

2. Müller, W. E. G., X. Wang, K. Kropf, H. Ushijima, W. Geurtsen, C. Eckert, M. N. Tahir, W. Tremel, A. Boreiko, U. Schloßmacher, J. Li, and H. C. Schröder, "Bioorganic/inorganic hybrid composition of sponge spicules: Matrix of the giant spicules and of the comitalia of the deep sea hexactinellid Monorhaphis," *Journal of Structural Biology*, Vol. 161, no. 2, pp. 188–203, 2008.

3. Amini, A. R., C. T. Laurencin, and S. P. Nukavarapu, "Bone tissue engineering: recent advances and challenges.," *Critical reviews in biomedical engineering*, Vol. 40, no. 5, p. 2, 2012.

4. Lu, Z., S. I. Roohani-Esfahani, G. Wang, and H. Zreiqat, "Bone biomimetic microenvironment induces osteogenic differentiation of adipose tissue-derived mesenchymal stem cells," *Nanomedicine: Nanotechnology, Biology, and Medicine*, Vol. 8, no. 4, pp. 507–515, 2012.

5. Kalfas, I. H., "Principles of bone healing," *Neurosurgical focus*, Vol. 10, no. 4, p. E1, 2001.

6. Dimar, J. R., and S. D. Glassman, "The art of bone grafting," *Current Opinion in Orthopaedics*, Vol. 18, no. 3, pp. 226–233, 2007.

7. Gravel, M., T. Gross, R. Vago, and M. Tabrizian, "Responses of mesenchymal stem cell to chitosan-coralline composites microstructured using coralline as gas forming agent," *Biomaterials*, Vol. 27, no. 9, pp. 1899–1906, 2006.

8. Langer, R., and J. P. Vacanti, "Tissue engineering.," *Science (New York, N.Y.)*, Vol. 260, no. 5110, pp. 920–6, 1993.

9. Narayanan, G., V. N. Vernekar, E. L. Kuyinu, and C. T. Laurencin, "Poly (lactic acid)-based biomaterials for orthopedic regenerative engineering," *Advanced Drug Delivery Reviews*, 2016.

10. Fuchs, E., and J. a. Segre, "Stem cells: a new lease on life.," *Cell*, Vol. 100, no. 1, pp. 143–155, 2000.

11. Caplan, A. I., "Adult mesenchymal stem cells for tissue engineering versus regenerative medicine," 2007.

12. US Department of Health and Human Services, "Bone health and osteoporosis: a report of the Surgeon General," *US Health and Human Services*, p. 437, 2004.

13. Porter, J. R., T. T. Ruckh, and K. C. Popat, "Bone Tissue Engineering : A Review in Bone Biomimetics and Drug Delivery Strategies," 2009.

14. Buckwalter, J., M. Glimcher, R. Cooper, and R. Recker, "Bone biology. I: Structure, blood supply, cells, matrix, and mineralization.," *Instructional Course Lectures*, Vol. 45, pp. 371–86, 1996.

15. Downey, P. a., and M. I. Siegel, "Bone biology and the clinical implications for osteoporosis.," *Physical therapy*, Vol. 86, no. 1, pp. 77–91, 2006.

16. Robling, A. G., A. B. Castillo, and C. H. Turner, "BIOMECHANICAL AND MOLECULAR REGULATION OF BONE REMODELING," *Annual Review of Biomedical Engineering*, no. 8, pp. 455–98, 2006.

17. Datta, H. K., W. F. Ng, J. a. Walker, S. P. Tuck, and S. S. Varanasi, "The cell biology of bone metabolism.," *Journal of clinical pathology*, Vol. 61, no. 5, pp. 577–587, 2008.

18. Clarke, B., "Normal bone anatomy and physiology.," 2008.

19. Karsenty, G., H. M. Kronenberg, and C. Settembre, "Genetic control of bone formation.," *Annual review of cell and developmental biology*, Vol. 25, pp. 629–48, 2009.

20. Everts, V., J. M. Delaissé, W. Korper, D. C. Jansen, W. Tigchelaar-Gutter, P. Saftig, and W. Beertsen, "The bone lining cell: its role in cleaning Howship's lacunae and initiating bone formation.," *Journal of bone and mineral research*, Vol. 17, no. 1, pp. 77–90, 2002.

21. Rho, J. Y., L. Kuhn-Spearing, and P. Zioupos, "Mechanical properties and the hierarchical structure of bone," *Medical Engineering and Physics*, Vol. 20, no. 2, pp. 92–102, 1998.

22. Laurencin, C. T., Y. Khan, M. Kofron, S. El-Amin, E. Botchwey, X. Yu, and J. a. Cooper, "The ABJS Nicolas Andry Award: Tissue engineering of bone and ligament: a 15-year perspective.," *Clinical orthopaedics and related research*, Vol. 447, no. 442, pp. 221–236, 2006.

23. Hunziker, E. B., "Articular cartilage repair: Basic science and clinical progress. A review of the current status and prospects," 2002.

24. Sims, N. A., and J. H. Gooi, "Bone remodeling: Multiple cellular interactions required for coupling of bone formation and resorption," 2008.

25. Matsuo, K., and N. Irie, "Osteoclast-osteoblast communication," 2008.

26. Frost, H. M., "Tetracycline-based histological analysis of bone remodeling," *Calcified Tissue Research*, Vol. 3, no. 1, pp. 211–237, 1969.

27. Hauge, E. M., D. Qvesel, E. F. Eriksen, L. Mosekilde, and F. Melsen, "Cancellous bone remodeling occurs in specialized compartments lined by cells expressing osteoblastic markers.," *Journal of bone and mineral research : the official journal of the American Society for Bone and Mineral Research*, Vol. 16, no. 9, pp. 1575–1582, 2001.

28. Andersen, T. L., T. E. Sondergaard, K. E. Skorzynska, F. Dagnaes-Hansen, T. L. Plesner, E. M. Hauge, T. Plesner, and J.-M. Delaisse, "A physical mechanism for coupling bone resorption and formation in adult human bone.," *The American journal of pathology*, Vol. 174, no. 1, pp. 239–247, 2009.

29. Dallas, S. L., M. Prideaux, and L. F. Bonewald, "The osteocyte: An endocrine cell . . . and more," 2013.

30. Callewaert, F., K. Venken, S. Boonen, and D. Vanderschueren, "Estrogen and the Skeleton - Rodents," in *Osteoporosis in Men*, pp. 283–287, 2010.

31. Sobacchi, C., A. Schulz, F. P. Coxon, A. Villa, and M. H. Helfrich, "Osteopetrosis: genetics, treatment and new insights into osteoclast function.," *Nature reviews. Endocrinology*, Vol. 9, no. 9, pp. 522–36, 2013.

32. Florencio-Silva, R., G. R. D. S. Sasso, E. Sasso-Cerri, M. J. Simões, and P. S. Cerri, "Biology of Bone Tissue: Structure, Function, and Factors That Influence Bone Cells," *BioMed Research International*, Vol. 2015, pp. 1–17, 2015.

33. Phan, T. C. A., J. Xu, and M. H. Zheng, "Interaction between osteoblast and osteoclast: Impact in bone disease," 2004.

34. Crockett, J. C., D. J. Mellis, D. I. Scott, and M. H. Helfrich, "New knowledge on critical osteoclast formation and activation pathways from study of rare genetic diseases of osteoclasts: Focus on the RANK/RANKL axis," 2011.

35. Redlich, K., and J. S. Smolen, "Inflammatory bone loss: pathogenesis and therapeutic intervention," *Nature Reviews Drug Discovery*, Vol. 11, no. 3, pp. 234–250, 2012.

36. Baroli, B., "From natural bone grafts to tissue engineering therapeutics: Brainstorming on pharmaceutical formulative requirements and challenges," 2009.

37. Frazer, K. A., S. S. Murray, N. J. Schork, and E. J. Topol, "Human genetic variation and its contribution to complex traits.," *Nature reviews. Genetics*, Vol. 10, no. 4, pp. 241–51, 2009.

38. Banwart, J. C., M. a. Asher, and R. S. Hassanein, "Iliac crest bone graft harvest donor site morbidity. A statistical evaluation.," *Spine*, Vol. 20, no. 9, pp. 1055–60, 1995.

39. Ebraheim, N. a., H. Elgafy, and R. Xu, "Bone-graft harvesting from iliac and fibular donor sites: techniques and complications.," *The Journal of the American Academy of Orthopaedic Surgeons*, Vol. 9, no. 3, pp. 210–218, 2001.

40. St John, T. A., A. R. Vaccaro, A. P. Sah, M. Schaefer, S. C. Berta, T. Albert, and A. Hilibrand, "Physical and monetary costs associated with autogenous bone graft harvesting.," *American journal of orthopedics (Belle Mead, N.J.)*, Vol. 32, no. 1, pp. 18–23, 2003.

41. Delloye, C., O. Cornu, V. Druez, and O. Barbier, "Bone allografts: What they can offer and what they cannot.," *The Journal of bone and joint surgery. British volume*, Vol. 89, no. 5, pp. 574–579, 2007.

42. Lord, C. F., M. C. Gebhardt, W. W. Tomford, and H. J. Mankin, "Infection in bone allografts. Incidence, nature, and treatment.," *The Journal of bone and joint surgery. American volume*, Vol. 70, no. 3, pp. 369–376, 1988.

43. Tomford, W. W., R. J. Starkweather, and M. H. Goldman, "A study of the clinical incidence of infection in the use of banked allograft bone.," *The Journal of bone and joint surgery. American volume*, Vol. 63, no. 2, pp. 244–8, 1981.

44. Greenwald, A. S., S. D. Boden, V. M. Goldberg, Y. Khan, C. T. Laurencin, and R. N. Rosier, "Bone-graft substitutes: facts, fictions, and applications.," *The Journal of bone and joint surgery. American volume*, Vol. 83-A Suppl, pp. 98–103, 2001.

45. Collignon, P., and L. Purdy, "Xenografts: Are the risks so great that we should not proceed?," 2001.

46. Griffith, L. G., and M. A. Swartz, "Capturing complex 3D tissue physiology in vitro.," *Nature reviews Molecular cell biology*, Vol. 7, no. 3, pp. 211–24, 2006.

47. Lalan, S., I. Pomerantseva, and J. P. Vacanti, "Tissue engineering and its potential impact on surgery," *World Journal of Surgery*, Vol. 25, no. 11, pp. 1458–1466, 2001.

48. Vert, M., Y. Doi, K.-H. Hellwich, M. Hess, P. Hodge, P. Kubisa, M. Rinaudo, and F. Schué, "Terminology for biorelated polymers and applications (IUPAC Recommendations 2012)," *Pure and Applied Chemistry*, Vol. 84, no. 2, p. 1, 2012.

49. Williams, D. F., "On the nature of biomaterials," *Biomaterials*, Vol. 30, no. 30, pp. 5897–5909, 2009.

50. Velasco, M. A., C. A. Narv??ez-Tovar, and D. A. Garz??n-Alvarado, "Design, materials, and mechanobiology of biodegradable scaffolds for bone tissue engineering," *BioMed Research International*, Vol. 2015, 2015.

51. Mitra, J., G. Tripathi, A. Sharma, and B. Basu, "Scaffolds for bone tissue engineering: role of surface patterning on osteoblast response," *RSC Advances*, Vol. 3, no. 28, p. 11073, 2013.

52. Place, E. S., J. H. George, C. K. Williams, and M. M. Stevens, "Synthetic polymer scaffolds for tissue engineering.," *Chemical Society reviews*, Vol. 38, no. 4, pp. 1139–1151, 2009.

53. Jones, J. I., and D. R. Clemmons, "Insulin-like growth factors and their binding proteins: Biological actions," 1995.

54. Miyazono, K., "Signal transduction by bone morphogenetic protein receptors: Functional roles of Smad proteins," 1999.

55. Heldin, C. H., K. Miyazono, and P. ten Dijke, "TGF-beta signalling from cell membrane to nucleus through SMAD proteins.," *Nature*, Vol. 390, no. 6659, pp. 465–71, 1997.

56. Huang, Z., E. R. Nelson, R. L. Smith, and S. B. Goodman, "The sequential expression profiles of growth factors from osteoprogenitors [correction of osteroprogenitors] to osteoblasts in vitro.," *Tissue engineering*, Vol. 13, no. 9, pp. 2311–20, 2007.

57. Phillips, A. M., "Overview of the fracture healing cascade.," *Injury*, Vol. 36 Suppl 3, no. 3, pp. S5–7, 2005.

58. Einhorn, T. a., "The cell and molecular biology of fracture healing.," *Clinical orthopaedics and related research*, no. 355 Suppl, pp. S7–S21, 1998.

59. Malizos, K. N., and L. K. Papatheodorou, "The healing potential of the periosteum molecular aspects.," *Injury*, Vol. 36 Suppl 3, pp. S13–S19, 2005.

60. Luginbuehl, V., L. Meinel, H. P. Merkle, and B. Gander, "Localized delivery of growth factors for bone repair.," *European journal of pharmaceutics and biopharmaceutics : official journal of Arbeitsgemeinschaft fur Pharmazeutische Verfahrenstechnik e.V*, Vol. 58, no. 2, pp. 197–208, 2004.

61. Li, R. H., and J. M. Wozney, "Delivering on the promise of bone morphogenetic proteins," 2001.

62. Bernstein, H. S., and D. Srivastava, "Stem cell therapy for cardiac disease," *Pediatric Research*, Vol. 71, no. 4-2, pp. 491–499, 2012.

63. Naderi, H., M. M. Matin, and a. R. Bahrami, "Review paper: Critical Issues in Tissue Engineering: Biomaterials, Cell Sources, Angiogenesis, and Drug Delivery Systems," *Journal of Biomaterials Applications*, Vol. 26, no. 4, pp. 383–417, 2011.

64. Takahashi, K., and S. Yamanaka, "Induction of pluripotent stem cells from mouse embryonic and adult fibroblast cultures by defined factors," *Cell*, Vol. 126, no. 4, pp. 663–676, 2006.

65. Yu, J., M. A. Vodyanik, K. Smuga-Otto, J. Antosiewicz-Bourget, J. L. Frane, S. Tian, J. Nie, G. A. Jonsdottir, V. Ruotti, R. Stewart, I. I. Slukvin, and J. A. Thomson, "Induced pluripotent stem cell lines derived from human somatic cells.," *Science (New York, N.Y.)*, Vol. 318, no. 5858, pp. 1917–20, 2007.

66. Zhu, Z., and D. Huangfu, "Human pluripotent stem cells: an emerging model in developmental biology.," *Development (Cambridge, England)*, Vol. 140, no. 4, pp. 705–17, 2013.

67. Nishikawa, S.-i., R. a. Goldstein, and C. R. Nierras, "The promise of human induced pluripotent stem cells for research and therapy.," *Nature reviews. Molecular cell biology*, Vol. 9, no. 9, pp. 725–729, 2008.

68. Zuk, P. a., M. Zhu, H. Mizuno, J. Huang, J. W. Futrell, a. J. Katz, P. Benhaim, H. P. Lorenz, and M. H. Hedrick, "Multilineage cells from human adipose tissue: implications for cell-based therapies.," *Tissue engineering*, Vol. 7, no. 2, pp. 211–228, 2001.

69. Martin, R. J., G. J. Hausman, and D. B. Hausman, "Regulation of adipose cell development in utero," *Proc Soc Exp Biol Med*, Vol. 219, no. 3, pp. 200–210, 1998.

70. Weisberg, S. P., D. McCann, M. Desai, M. Rosenbaum, R. L. Leibel, and A. W. Ferrante, "Obesity is associated with macrophage accumulation in adipose tissue," *Journal of Clinical Investigation*, Vol. 112, no. 12, pp. 1796–1808, 2003.

71. Xu, H., G. Barnes, Q. Yang, G. Tan, D. Yang, C. Chou, J. Sole, A. Nichols, J. Ross, L. Tartaglia, and Others, "Chronic inflammation in fat plays a crucial role in the development of obesity-related insulin resistance," *Journal of Clinical Investigation*, Vol. 112, no. 12, pp. 1821–1830, 2003.

72. Keung, E. Z., P. J. Nelson, and C. Conrad, "Concise review: genetically engineered stem cell therapy targeting angiogenesis and tumor stroma in gastrointestinal malignancy.," *Stem cells (Dayton, Ohio)*, Vol. 31, no. 2, pp. 227–35, 2013.

73. Lindroos, B., R. Suuronen, and S. Miettinen, "The potential of adipose stem cells in regenerative medicine," *Stem cell reviews*, Vol. 7, no. September, pp. 269–291, 2011.

74. Illouz, Y. G., "Body contouring by lipolysis: a 5-year experience with over 3000 cases.," *Plastic and reconstructive surgery*, Vol. 72, no. 5, pp. 591–597, 1983.

75. Sterodimas, A., J. de Faria, B. Nicaretta, and I. Pitanguy, "Tissue engineering with adipose-derived stem cells (ADSCs): current and future applications.," *Journal of plastic, reconstructive & aesthetic surgery : JPRAS*, Vol. 63, no. 11, pp. 1886–1892, 2010.

76. Demir, Ö., "Bone Surface Microenvironment Mimicked Biodegredable Polimeric Scaffolds," *Master's thesis, Bogazici University, Istanbul, Turkey*, 2011.

77. Özgürbüz, L. M., "Production of xenografts for hard tissue repair," *Master's thesis, Hacettepe University, Ankara, Turkey*, 2006.

78. Mima, Y., S. Fukumoto, H. Koyama, M. Okada, S. Tanaka, T. Shoji, M. Emoto, T. Furuzono, Y. Nishizawa, and M. Inaba, "Enhancement of cell-based therapeutic angiogenesis using a novel type of injectable scaffolds of hydroxyapatite-polymer nanocomposite microspheres," *PLoS ONE*, Vol. 7, no. 4, 2012.

79. Wen, F., S. Chang, Y. C. Toh, S. H. Teoh, and H. Yu, "Development of poly (lactic-co-glycolic acid)-collagen scaffolds for tissue engineering," *Materials Science and Engineering C*, Vol. 27, no. 2, pp. 285–292, 2007.

80. Fa??bender, M., S. Minkwitz, C. Strobel, G. Schmidmaier, and B. Wildemann, "Stimulation of bone healing by sustained bone morphogenetic protein 2 (BMP-2) delivery," *International Journal of Molecular Sciences*, Vol. 15, no. 5, pp. 8539–8552, 2014.

81. Ma, H., W. Su, Z. Tai, D. Sun, X. Yan, B. Liu, and Q. Xue, "Preparation and cytocompatibility of polylactic acid/hydroxyapatite/graphene oxide nanocomposite fibrous membrane," *Chinese Science Bulletin*, Vol. 57, no. 23, pp. 3051–3058, 2012.

82. Nejati, E., V. Firouzdor, M. B. Eslaminejad, and F. Bagheri, "Needle-like nano hydroxyapatite/poly(l-lactide acid) composite scaffold for bone tissue engineering application," *Materials Science and Engineering C*, Vol. 29, no. 3, pp. 942–949, 2009.

83. Rim, N. G., S. J. Kim, Y. M. Shin, I. Jun, D. W. Lim, J. H. Park, and H. Shin, "Mussel-inspired surface modification of poly(l-lactide) electrospun fibers for modulation of osteogenic differentiation of human mesenchymal stem cells," *Colloids and Surfaces B: Biointerfaces*, Vol. 91, no. 1, pp. 189–197, 2012.

84. Liu, Y., D. A. Peterson, H. Kimura, and D. Schubert, "Mechanism of cellular 3-(4,5-dimethylthiazol-2-yl)-2,5-diphenyltetrazolium bromide (MTT) reduction.," *Journal of neurochemistry*, Vol. 69, no. 2, pp. 581–93, 1997.

85. Lao, L., Y. Wang, Y. Zhu, Y. Zhang, and C. Gao, "Poly(lactide-co-glycolide)/hydroxyapatite nanofibrous scaffolds fabricated by electrospinning for bone tissue engineering," *Journal of Materials Science: Materials in Medicine*, Vol. 22, no. 8, pp. 1873–1884, 2011.

86. Faezeh Alipour, D. V. M., D. V. M. Abbas Parham, D. V. M. Hossein Kazemi Mehrjerdi, and D. V. M. Hesam Dehghani, "Equine adipose-Derived mesenchymal stem cells: Phenotype and growth characteristics, gene expression profile and differentiation potentials," *Cell Journal*, Vol. 16, no. 4, pp. 456–465, 2015.

87. Guilak, F., K. E. Lott, H. A. Awad, Q. Cao, K. C. Hicok, B. Fermor, and J. M. Gimble, "Clonal analysis of the differentiation potential of human adipose-derived adult stem cells," *Journal of Cellular Physiology*, Vol. 206, no. 1, pp. 229–237, 2006.

88. Song, K., Z. Yang, T. Liu, W. Zhi, X. Li, L. Deng, Z. Cui, and X. Ma, "Fabrication and detection of tissue-engineered bones with bio-derived scaffolds in a rotating bioreactor.," *Biotechnology and applied biochemistry*, Vol. 45, no. Pt 2, pp. 65–74, 2006.

89. Song, K., T. Liu, Z. Cui, X. Li, and X. Ma, "Three-dimensional fabrication of engineered bone with human bio-derived bone scaffolds in a rotating wall vessel bioreactor," *Journal of Biomedical Materials Research - Part A*, Vol. 86, no. 2, pp. 323–332, 2008.

90. Ng, K., E. Romas, L. Donnan, and D. M. Findlay, "Bone biology," Vol. 11, no. 1, 1997.

91. Wennerberg, A., and T. Albrektsson, "Effects of titanium surface topography on bone integration: A systematic review," 2009.

92. Qin, Z., A. Gautieri, A. K. Nair, H. Inbar, and M. J. Buehler, "Thickness of hydroxyapatite nanocrystal controls mechanical properties of the collagen-hydroxyapatite interface," *Langmuir*, Vol. 28, no. 4, pp. 1982–1992, 2012.

93. Ahn, H. H., I. W. Lee, H. B. Lee, and M. S. Kim, "Cellular behavior of human adipose-derived stem cells on wettable gradient polyethylene surfaces," *International Journal of Molecular Sciences*, Vol. 15, no. 2, pp. 2075–2086, 2014.

94. Abdal-Hay, A., F. A. Sheikh, and J. K. Lim, "Air jet spinning of hydroxyapatite/poly(lactic acid) hybrid nanocomposite membrane mats for bone tissue engineering," *Colloids and Surfaces B: Biointerfaces*, Vol. 102, pp. 635–643, 2013.

95. Tanimoto, Y., and N. Nishiyama, "Preparation and In Vitro Behavior of a Poly (lactic acid) -Fiber / Hydroxyapatite Composite Sheet," Vol. 2009, 2009.

96. Deplaine, H., M. Lebourg, P. Ripalda, A. Vidaurre, P. Sanz-Ramos, G. Mora, F. Prõsper, I. Ochoa, M. Doblaré, J. L. Gõmez Ribelles, I. Izal-Azcárate, and G. Gallego Ferrer, "Biomimetic hydroxyapatite coating on pore walls improves osteointegration of poly(L-lactic acid) scaffolds," *Journal of Biomedical Materials Research - Part B Applied Biomaterials*, Vol. 101 B, no. 1, pp. 173–186, 2013.

97. Beamson, G., and D. Briggs, "High resolution monochromated X-ray photoelectron spectroscopy of organic polymers: A comparison between solid state data for organic polymers and gas phase data for small molecules," *Molecular Physics*, Vol. 76, no. 4, pp. 919–936, 1992.

98. Paragkumar N, T., D. Edith, and J. L. Six, "Surface characteristics of PLA and PLGA films," *Applied Surface Science*, Vol. 253, no. 5, pp. 2758–2764, 2006.

99. Mas, B. A., S. Mara de Mello Cattani, R. de Cassia Cipriano Rangel, G. De Almeida Ribeiro, N. C. Cruz, F. De Lima Leite, P. A. De Paula Nascente, and E. A. De Rezende Duek, "Surface Characterization and Osteoblast-like Cells Culture on Collagen Modified PLDLA Scaffolds," *Materials Research*, Vol. 17, no. 6, pp. 1523–1534, 2014.

100. Cui, M., L. Liu, N. Guo, R. Su, and F. Ma, "Preparation, Cell Compatibility and Degradability of Collagen-Modified Poly(lactic acid)," pp. 595–607, 2015.

101. Hoidy, W. H., M. B. Ahmad, E. A. J. Al-Mulla, and N. A. B. Ibrahim, "Preparation and characterization of polylactic acid/polycaprolactone clay nanocomposites," *Journal of Applied Sciences*, Vol. 10, no. 2, pp. 97–106, 2010.

102. Eslami, H., M. Solati-Hashjin, and M. Tahriri, "Synthesis and Characterization of Hydroxyapatite Nanocrystals via Chemical Precipitation Technique," *Iranian Journal of Pharmaceutical Sciences SPring*, Vol. 4, no. 2, pp. 127–134, 2008.

103. Twardowski, J., *Raman and IR spectroscopy in biology and biochemistry / J. Twardowski, P. Anzenbacher ; translation editor, Mary Masson*, Ellis Horwood series in analytical chemistry, New York : Warsaw: Ellis Horwood ; Polish Scientific Publishers, 1994.

104. Lazarev, Y. A., B. A. Grishkovsky, and T. B. Khromova, "Amide I Band of IR Spectrum and Structure of Collagen and Related Polypeptides," *Biopolymers*, Vol. 24, pp. 1449–1478, 1985.

105. Tiong, W. H. C., G. Damodaran, H. Naik, J. L. Kelly, and A. Pandit, "Enhancing amine terminals in an amine-deprived collagen matrix," *Langmuir*, Vol. 24, no. 20, pp. 11752–11761, 2008.

106. Chen, C.-Y., C.-J. Ke, K.-C. Yen, H.-C. Hsieh, J.-S. Sun, and F.-H. Lin, "3D porous calcium-alginate scaffolds cell culture system improved human osteoblast cell clusters for cell therapy.," *Theranostics*, Vol. 5, no. 6, pp. 643–55, 2015.

107. Sayin, E., E. T. Baran, and V. Hasirci, "Osteogenic differentiation of adipose derived stem cells on high and low aspect ratio micropatterns," Vol. 5063, no. March 2016, 2015.

108. Puvaneswary, S., H. B. Raghavendran, S. Talebian, M. R. Murali, S. A Mahmod, S. Singh, and T. Kamarul, "Incorporation of Fucoidan in β-Tricalcium phosphate-Chitosan scaffold prompts the differentiation of human bone marrow stromal cells into osteogenic lineage," *Scientific Reports*, Vol. 6, no. April, p. 24202, 2016.

109. Osamu, S., N. Masanori, M. Yoshinori, K. Manabu, and S. Minoru, "Bone Formation on Synthetic Precursors of Hydroxyapatite," *Tohoku J. Exp. Med.*, Vol. 164, pp. 37–50, 1991.

110. Navarro-pardo, F., G. Martínez-barrera, A. L. Martínez-hernández, V. M. Castaño, J. L. Rivera-armenta, and F. Medellín-rodríguez, "Effects on the Thermo-Mechanical and Crystallinity Properties of Nylon 6,6 Electrospun Fibres Reinforced with One Dimensional (1D) and Two Dimensional (2D) Carbon," no. April, pp. 3494–3513, 2013.

111. Schroeder, J. E., and R. Mosheiff, "Tissue engineering approaches for bone repair : Concepts and evidence," *Injury*, Vol. 42, no. 6, pp. 609–613, 2011.

112. Kulkarni, R. K., E. G. Moore, A. F. Hegyeli, and F. Leonard, "Biodegradable Poly(lactic acid) Polymers," Vol. 5, pp. 169–181, 1971.

113. Tian, T., D. Jiang, J. Zhang, and Q. Lin, "Fabrication of bioactive composite by developing PLLA onto the framework of sintered HA scaffold," *Materials Science and Engineering C*, Vol. 28, no. 1, pp. 51–56, 2008.

114. Tsuji, K., A. Bandyopadhyay, B. D. Harfe, K. Cox, S. Kakar, L. Gerstenfeld, T. Einhorn, C. J. Tabin, and V. Rosen, "BMP2 activity, although dispensable for bone formation, is required for the initiation of fracture healing.," *Nature genetics*, Vol. 38, no. 12, pp. 1424–1429, 2006.

115. Schofer, M. D., S. Fuchs-winkelmann, C. Gräbedünkel, C. Wack, R. Dersch, M. Rudisile, J. H. Wendorff, A. Greiner, J. R. J. Paletta, and U. Boudriot, "Influence of Poly (L-Lactic Acid) Nanofibers and BMP-2- Containing Poly (L-Lactic Acid) Nanofibers on Growth and Osteogenic Differentiation of Human Mesenchymal Stem Cells," pp. 1269–1279, 2008.

116. Burkus, J. K., S. E. Heim, M. F. Gornet, and T. A. Zdeblick, "Is INFUSE bone graft superior to autograft bone? An integrated analysis of clinical trials using the LT-CAGE lumbar tapered fusion device," *J Spinal Disord Tech*, Vol. 16, no. 2, pp. 113–122, 2003.

117. Sawyer, A. A., S. J. Song, E. Susanto, P. Chuan, C. X. F. Lam, M. A. Woodruff, D. W. Hutmacher, and S. M. Cool, "The stimulation of healing within a rat calvarial defect by mPCL-TCP/collagen scaffolds loaded with rhBMP-2," *Biomaterials*, Vol. 30, no. 13, pp. 2479–2488, 2009.

118. Wang, P., L. Zhao, J. Liu, M. D. Weir, X. Zhou, and H. H. K. Xu, "Bone tissue engineering via nanostructured calcium phosphate biomaterials and stem cells," no. July, 2014.

119. Wang, H., G. Wu, J. Zhang, K. Zhou, B. Yin, X. Su, G. Qiu, G. Yang, X. Zhang, G. Zhou, and Z. Wu, "Osteogenic effect of controlled released rhBMP-2 in 3D printed porous hydroxyapatite scaffold," *Colloids and Surfaces B: Biointerfaces*, Vol. 141, pp. 491–498, 2016.

120. Adachi, T., Y. Osako, M. Tanaka, M. Hojo, and S. J. Hollister, "Framework for optimal design of porous scaffold microstructure by computational simulation of bone regeneration," *Biomaterials*, Vol. 27, no. 21, pp. 3964–3972, 2006.

121. Lin, C. Y., N. Kikuchi, and S. J. Hollister, "A novel method for biomaterial scaffold internal architecture design to match bone elastic properties with desired porosity," *Journal of Biomechanics*, Vol. 37, no. 5, pp. 623–636, 2004.

122. Kamath, M. S., S. S. S. J. Ahmed, M. Dhanasekaran, and S. W. Santosh, "Bone Regeneration Based on Tissue Engineering Conceptions - A 21st Century Perspective," *International journal of nanomedicine*, Vol. 9, no. 1, pp. 183–95, 2014.

123. Kleinheinz, J., S. Jung, K. Wermker, C. Fischer, and U. Joos, "Release kinetics of VEGF165 from a collagen matrix and structural matrix changes in a circulation model," *Head Face Med*, Vol. 6, p. 17, 2010.

124. Helena, M., and H. Sander, "Low-cost Processing Technology for the Synthesis of Calcium Phosphates / Collagen Biocomposites for Potential Bone Tissue Engineering Applications 2 . Experimental Procedure," Vol. 10, no. 4, pp. 431–436, 2007.

125. Schaub, N. J., C. Le Beux, J. Miao, R. J. Linhardt, J. G. Alauzun, D. Laurencin, and R. J. Gilbert, "The effect of surface modification of aligned poly-l-lactic acid electrospun fibers on fiber degradation and neurite extension," *PLoS ONE*, Vol. 10, no. 9, 2015.

126. Ma, Z., C. Gao, J. Ji, and J. Shen, "Protein immobilization on the surface of poly- L -lactic acid films for improvement of cellular interactions," Vol. 38, pp. 2279–2284, 2002.

127. Wenzel, R. N., "Surface Roughness and Contact Angle.," *Journal of Psychosomatic Research*, Vol. 30, no. 3, p. 387, 1986.

128. Abdallah, B. M., and M. Kassem, "Human mesenchymal stem cells : from basic biology to clinical applications," Vol. 106, pp. 109–116, 2008.

129. Hutmacher, D. W., "Sca ! olds in tissue engineering bone and cartilage," Vol. 21, pp. 2529–2543, 2000.

130. Yilgor, P., R. A. Sousa, R. L. Reis, N. Hasirci, and V. Hasirci, "Effect of scaffold architecture and BMP-2/BMP-7 delivery on in vitro bone regeneration," *Journal of Materials Science: Materials in Medicine*, Vol. 21, no. 11, pp. 2999–3008, 2010.

131. Palin, E., H. Liu, and T. J. Webster, "Mimicking the nanofeatures of bone increases bone-forming cell adhesion and proliferation," *Nanotechnology*, Vol. 16, no. 9, p. 1828, 2005.

132. Hassenkam, T., G. E. Fantner, J. A. Cutroni, J. C. Weaver, D. E. Morse, and P. K. Hansma, "High-resolution AFM imaging of intact and fractured trabecular bone," *Bone*, Vol. 35, no. 1, pp. 4–10, 2004.

133. Bottino, M. C., V. Thomas, and G. M. Janowski, "A novel spatially designed and functionally graded electrospun membrane for periodontal regeneration," *Acta Biomaterialia*, Vol. 7, no. 1, pp. 216–224, 2011.

134. Lv, Q., M. Deng, B. D. Ulery, L. S. Nair, and C. T. Laurencin, "Nano-ceramic composite scaffolds for bioreactor-based bone engineering basic research," in *Clinical Orthopaedics and Related Research*, Vol. 471, pp. 2422–2433, 2013.

135. Rizzi, S. C., D. J. Heath, A. G. A. Coombes, N. Bock, M. Textor, and S. Downes, "Biodegradable polymer/hydroxyapatite composites: Surface analysis and initial attachment of human osteoblasts," *Journal of Biomedical Materials Research*, Vol. 55, no. 4, pp. 475–486, 2001.

136. Ji, Y., G. P. Xu, J. L. Yan, and S. H. Pan, "Transplanted bone morphogenetic protein/poly(lactic-co-glycolic acid) delayed-release microcysts combined with rat micromorselized bone and collagen for bone tissue engineering.," *The Journal of international medical research*, Vol. 37, no. 4, pp. 1075–87, 2009.